FERMILAB-PUB-16-409-APC (accepted)

Prepared for submission to JINST

Observation of Electron Cloud Instabilities and Emittance Dilution at the Cornell Electron-Positron Storage Ring Test Accelerator

R.L. Holtzapple,[a,1] **M.G. Billing**[b] **R.C. Campbell**[a] **G.F. Dugan**[b] **J. Flanagan**[d]
K.E. McArdle[a] **M.I. Miller**[a] **M.A. Palmer**[c] **G. A. Ramirez**[b] **K.G. Sonnad**[b,d]
M.M. Totten[a] **S.L. Tucker**[a] **H. A. Williams**[b]

[a] *Physics Department, California Polytechnic State University, San Luis Obispo, CA 93407, U.S.A.*

[b] *Cornell Laboratory for Accelerator-based Sciences and Education, Cornell University, Ithaca, NY, 14850, U.S.A.*

[c] *Fermi National Accelerator Laboratory, Batavia, IL 60510, U.S.A.*

[d] *High Energy Accelerator Research Organization (KEK), Tsukuba, Ibaraki 305-0801, Japan.*

E-mail: rholtzap@calpoly.edu

Abstract: Electron cloud related emittance dilution and instabilities of bunch trains limit the performance of high intensity circular colliders. One of the key goals of the Cornell electron-positron storage ring Test Accelerator (CesrTA) research program is to improve our understanding of how the electron cloud alters the dynamics of bunches within the train. Single bunch beam diagnotics have been developed to measure the beam spectra, vertical beam size, two important dynamical effects of beams interacting with the electron cloud, for bunch trains on a turn-by-turn basis. Experiments have been performed at CesrTA to probe the interaction of the electron cloud with stored positron bunch trains. The purpose of these experiments was to characterize the dependence of beamâĂŞelectron cloud interactions on the machine parameters such as bunch spacing, vertical chromaticity, and bunch current. The beam dynamics of the stored beam, in the presence of the electron cloud, was quantified using: 1) a gated beam position monitor (BPM) and spectrum analyzer to measure the bunch-by-bunch frequency spectrum of the bunch trains; 2) an x-ray beam size monitor to record the bunch-by-bunch, turn-by-turn vertical size of each bunch within the trains. In this paper we report on the observations from these experiments and analyze the effects of the electron cloud on the stability of bunches in a train under many different operational conditions.

Keywords: Only keywords from JINST's keywords list please

[1]Corresponding author.

Operated by Fermi Research Alliance, LLC under Contract No. DE-AC02-07CH11359 with the United States Department of Energy.

Contents

1 Introduction

One of the key goals of the Cornell electron-positron storage ring Test Accelerator (CesrTA) research program is to improve our understanding of the interaction of the electron cloud with the high energy particle beam. This improved understanding is required to be able to extrapolate with confidence from the experimental conditions of CesrTA to the conditions expected for the ILC damping rings [**?**]. The interaction of the particle beam with the cloud can be studied by measuring the properties of the beam in the presence of the cloud. The key beam properties which are influenced by the cloud are the beam's closed orbit distortion (quite small, and not extensively studied with CesrTA), the frequency spectrum of the beam centroid's coherent dipole motion relative to this orbit, and the beam's transverse position distribution. In CesrTA the beam is formatted longitudinally into a train of ($\sim$ 10 mm long) bunches separated by an adjustable spacing (variable from a minimum of 4 ns, up to a maximum equal to the revolution period, about 2.56 μs). For sufficiently closely-spaced bunches, the electron cloud grows along the train. Because the cloud environment is different, it is critical that the beam dynamics measurement made to probe the cloud be done on a bunch-by-bunch basis. The frequency spectrum of the coherent dipole motion of each bunch contains a wealth of information. In particular this information includes

- the amplitude, frequency, and line shape of the betatron lines, which are sensitive to the electron cloud's electric field, to the mode of oscillation of the bunches in the train, and to the presence of multi-bunch instabilities;
- the amplitude, frequency, and line shape of "head-tail" lines, which are generally separated from the betatron lines by approximately the synchrotron frequency, and are sensitive to internal motion within the bunch driven by electron-cloud-induced single-bunch head-tail instabilities.

In addition after bunch motion has been excited by an external source, the time dependence of the amplitude of the betatron and "head-tail" lines provides information on the damping of these lines, which is related to aspects of the effective electron-cloud impedance not probed by tune measurements. The vertical shape distribution of each bunch is sensitive to

- emittance growth driven by single-bunch instabilities. Generally, this growth would be expected to be correlated with the observation of "head-tail" lines described in the previous paragraphs;
- incoherent emittance growth, driven by non-linear components of the electron cloud's electric field, which may take place before the onset of emittance growth driven by single-bunch coherent instabilities.

If present, incoherent emittance growth needs to be fully understood, since it could impact achieving the design emittance goals of the ILC damping rings and future lepton colliders and light sources. In this paper an overview of the experimental hardware and techniques used to obtain the measurements are described; the most important beam dynamics observations are presented; and a summary of the results are discussed.

2 Instability Thresholds: Experimental Measurements

We have developed the capability to make automated measurements of frequency spectra of individual bunches, to look for signals of single-bunch instabilities [**?**]-[**?**]. During such measurements for each bunch in a train several frequency spectra are acquired, covering a range which spans from one-half the revolution frequency to the revolution frequency. Machine conditions, such as bunch current, magnet settings, feedback system parameters, etc. are automatically recorded and stored before and after each single-bunch spectrum is taken.

Over the course of five years a number of observations were made which illuminate the dynamics of the electron-cloud/beam interaction at CesrTA. Some of the results from these experiments are described below.

Unless otherwise noted all experiments discussed in this section were done at 2.085 GeV in a low emittance lattice [**?**]. The machine parameters for these experiments are shown in Table I.

Table 1. Nominal machine parameters at 2.085 GeV. The emittances and tunes are those of a single bunch in the storage ring.

Parameter	**Value**	**Unit**
Energy	2.085	GeV
Lattice	2085mev_20090516	
Horizontal emittance	2.6	nm
Vertical emittance	~ 20	pm
Bunch length	10.8	mm
Horizontal tune	14.55	
Vertical tune	9.58	
Synchrotron tune	0.065	
Momentum compaction	6.8×10^{-3}	
Revolution frequency	390.13	kHz

Trains having a number of bunches ranging from 30 to 45, with a bunch spacing of 4 to 56 ns, and bunch currents in the range of $0.5 - 1.25$ mA ($0.8 - 2.0 \times 10^{10}$ particles) per bunch were studied. In all cases, except where specifically noted, the beam particles were positrons.

Several systematic checks were undertaken:

- Checks were made to rule out inter-modulation distortion in the Beam Position Monitor (BPM) electronics and to put a bound on the nonlinearities of the BPM itself [**?**].
- The betatron and synchro-betatron (head-tail) lines shifted in frequency as expected when the vertical, horizontal, and synchrotron tunes were varied.

Unless otherwise mentioned, the longitudinal feedback was off for these measurements. The vertical and horizontal bunch-by-bunch feedback systems' gains were turned down to 20% of full gain. Some experiments explored the effect of turning the vertical feedback fully off.

3 General observations

Even with horizontal and vertical feedback in operation coherent horizontal and vertical betatron motion is visible as spectral lines. Generally the amplitude of these lines increases as one moves the observation point from one bunch to the next within the train. Another basic observation is that under a variety of conditions the frequency spectra exhibit the vertical $m = \pm 1$ synchro-betatron (head-tail) lines, separated from the vertical betatron line by the synchrotron frequency, for many of the bunches along the train. The amplitude of these lines typically (but not always) grows along the train. Under some circumstances horizontal head-tail modes are also observed. The m=-1 signal refers to the lower sideband whereas the m=+1 signal refers to the upper sideband of the vertical betatron line.

Typically, for the bunch at which the vertical synchro-betatron lines first appear above the noise floor (which is about 40 dB below the vertical betatron line), we observe, on a bunch-by-bunch x-ray Beam Size Monitor (xBSM), growth in the beam size, which continues to increase along the train [**?**].

Under some conditions the first bunch in the train also exhibits a synchro-betatron line ($m = -1$ only). When we placed a "precursor" bunch, about 180 ns before the train, this $m = -1$ signal for the first bunch was eliminated.

Subsequent sections will present the details of these observations, together with their dependence on machine and beam parameters such as bunch current, number of bunches, chromaticity, beam emittance, vertical feedback, beam energy, and particle species.

3.1 Bunch-by-Bunch Power Spectrum

To measure a bunch-by-bunch power spectrum the machine is loaded with a bunch train with a uniform current per bunch and software is run to automatically collect frequency spectra from a single BPM button gated on the first bunch. The data acquisition takes less than a minute and then gate is moved to the second bunch and so on through the train. For bunch spacingâĂŹs greater than about 6 ns, the gate width is smaller than the bunch spacing, so only the motion of the gated bunch is observed. The frequency spectra are 10 s averages, acquired in 4 (or 5) measurements, each with a 40 kHz span, covering the range from 185 up to 345 (or 385) kHz. During a single measurement sequence all of these groups of spectra for the ensemble of bunches are collected into data sets. Since a large amount of data has been acquired over several years, for clarity this paper will reference measurements by their data set numbers. Since the beam has a relatively short lifetime, it is necessary to periodically pause the measurements and "top off" the bunch train. Typically, this is done after data acquisition is completed for a group of 5 bunches. Fig. **??** shows the beam current as a function of bunch number for a 30 bunch train. In this figure the current per bunch plotted for bunch n corresponds to the average value of the bunch current for all bunches earlier than bunch n; the error bar represents the rms variation in this number, principally due to

irregularities in the fill level. The dips at bunches 5, 10, . . ., and peaks at 6, 11, . . ., correspond to when the train is "topped off."

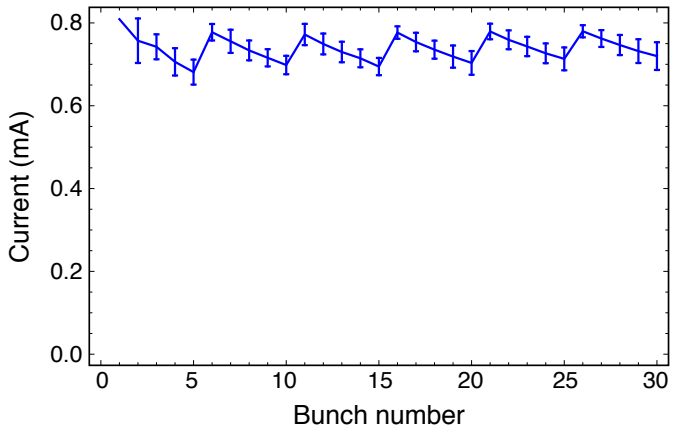

Figure 1. Bunch-by-bunch current during the measurement of the beam spectrum of a 30 bunch train. (From data set 166.)

A portion of the bunch-by-bunch power spectrum observed in data set 166, which consists of a 30 bunch train of positrons with 14 ns bunch spacing, is shown in Fig. **??**. The figure plots the power spectrum for each bunch, as measured at the button BPM, vs. frequency. The four prominent peaks seen correspond, from lowest to highest frequency, to the $m = -1$ vertical synchro-betatron line the horizontal betatron line, the vertical betatron line, and the $m = +1$ vertical synchro-betatron line. Fig. **??** shows the spectrum of the last bunch (number 30) in greater detail. For this data set the vertical chromaticity (defined as $Q\prime = \frac{dQ}{d\delta}$, where δ is the fractional momentum deviation and Q is the tune) was 1.16 and the horizontal chromaticity was 1.33 [**?**]. The principal features exhibited in Fig. **??** and Fig. **??** are discussed in more detail in the next subsections.

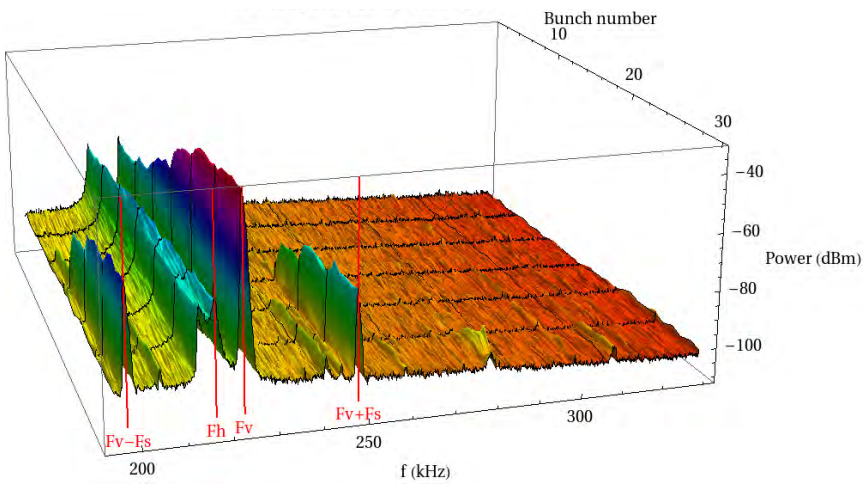

Figure 2. Bunch-by-bunch power spectrum along a 30 bunch train of positrons with 14 ns bunch spacing. (From data set 166.)

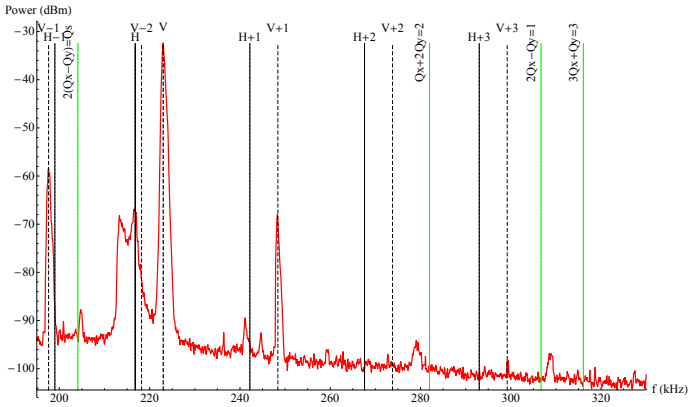

Figure 3. Power spectrum for bunch number 30 in a 30 bunch-long train. As an example the lines labeled "V+1" and "V-1" are shown at frequencies of $\pm f_s$ from the vertical betatron line ("V"), in which f_s is the synchrotron frequency. The locations of several storage ring resonances are also indicated. (From data set 166.)

3.2 Power Spectrum Features near the Betatron Lines

3.2.1 Horizontal Betatron Lineshape

Fig. **??** shows typical bunch-by-bunch power spectra near the horizontal betatron line for 8 ns and 14 ns bunch spacings. For both bunch spacings there is single peak visible at the beginning of the bunch train that splits as we move along the train into two peaks, a high and low amplitude peak. This tune splitting has been measured at bunch spacings between 4-20 ns. The high amplitude peak shifts up in frequency along the bunch train and is attributable to the electron cloud. This peak's frequency shift (or tune shift) increases when the bunch current increases, decreases when the bunch spacing increases and does not change when the vertical chromaticity is varied. In addition there is a lower amplitude "shoulder", which appears to be roughly constant in frequency during the bunch train (i.e., there is no tune shift). A plausible explanation for this shoulder is the following: For the coupled bunch mode when all the bunches in the train are oscillating in-phase, the horizontal tune shift due to the electron cloud in a dipole-dominated ring such as CESR is very small. However, for the data set shown in Fig. **??**, the bunches in the train are spontaneously excited, so a mixture of coupled bunch modes will be present. This mixture of coupled bunch modes will exhibit a spectrum of electron-cloud-induced tune shifts, ranging from nearly zero tune shift for the mode in which the bunches are oscillating in phase, to large tune shifts for modes in which bunches are oscillating with different phases [**?**]. Qualitatively, this should produce a spectrum similar to that shown in Fig. **??**.

3.2.2 Vertical Betatron Lineshape

Likewise, Fig. **??** shows typical bunch-by-bunch power spectra near the vertical betatron line for two different bunch spacings. At short bunch spacings, between 4-12 ns, there are two peaks near the vertical betatron line at the beginning of the bunch train. The high amplitude peak shifts up in frequency along the bunch train and is attributed to the electron cloud. This tune splitting has been measured when bunch spacings are between 4 to 14 ns. The frequency shift, of the high amplitude

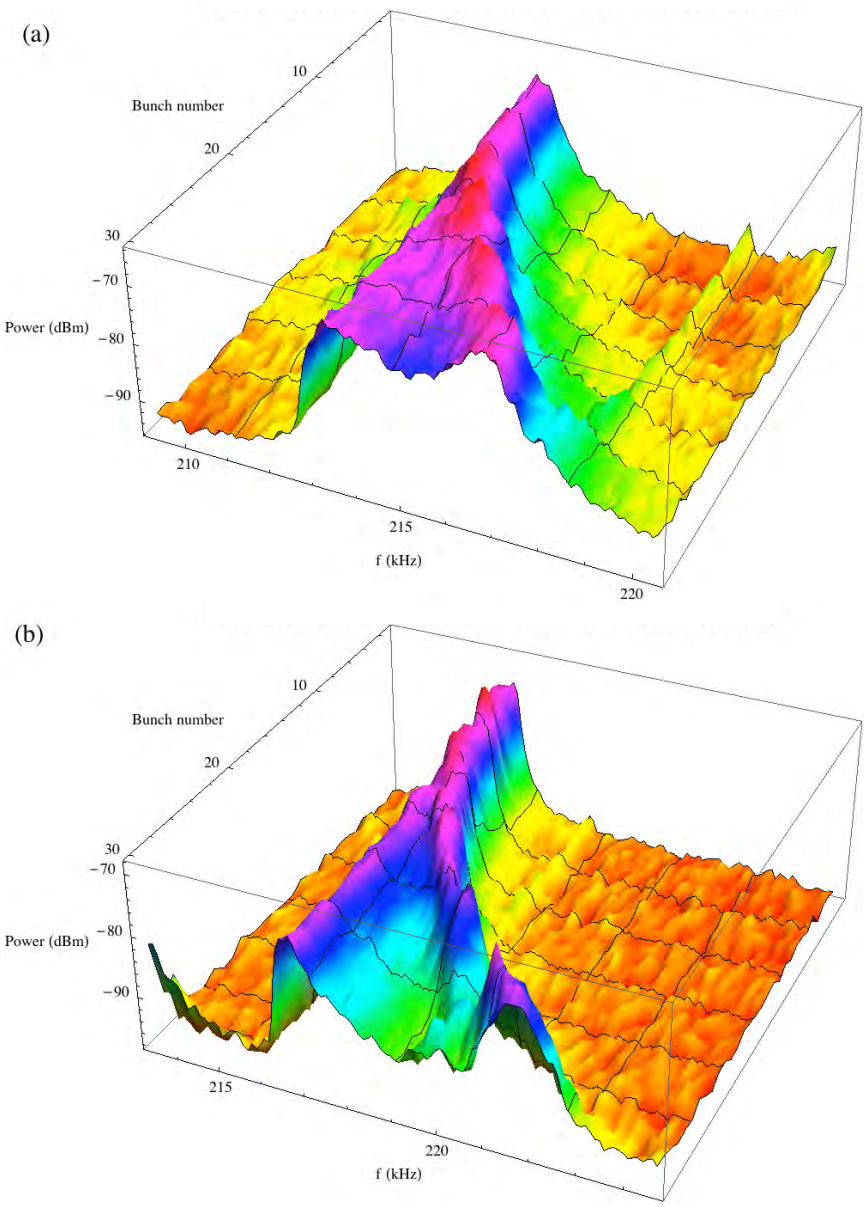

Figure 4. Bunch-by-bunch power spectra for the horizontal betatron line for bunches of 0.75 mA currents in 30 bunch trains with (a) 14 ns bunch spacing (data set 166) and (b) 8 ns bunch spacing (data set 964).

peaks, increases when the bunch current increases and decreases when bunch spacing increases. In addition there is a smaller peak at a higher frequency, present even for the first bunch, which appears to grow in amplitude and merge with the main peak near the end of the bunch train. Increasing the vertical chomaticity causes the small peak to merge into the high amplitude peak. Since this peak is present even for the first bunch, it is unlikely that it is a multibunch mode vertical tune shift due to the electron cloud. Also, measurements and simulations have shown that the dependence of the *vertical* tune shifts on the multibunch mode is much smaller than for the horizontal tune shifts [**?**].

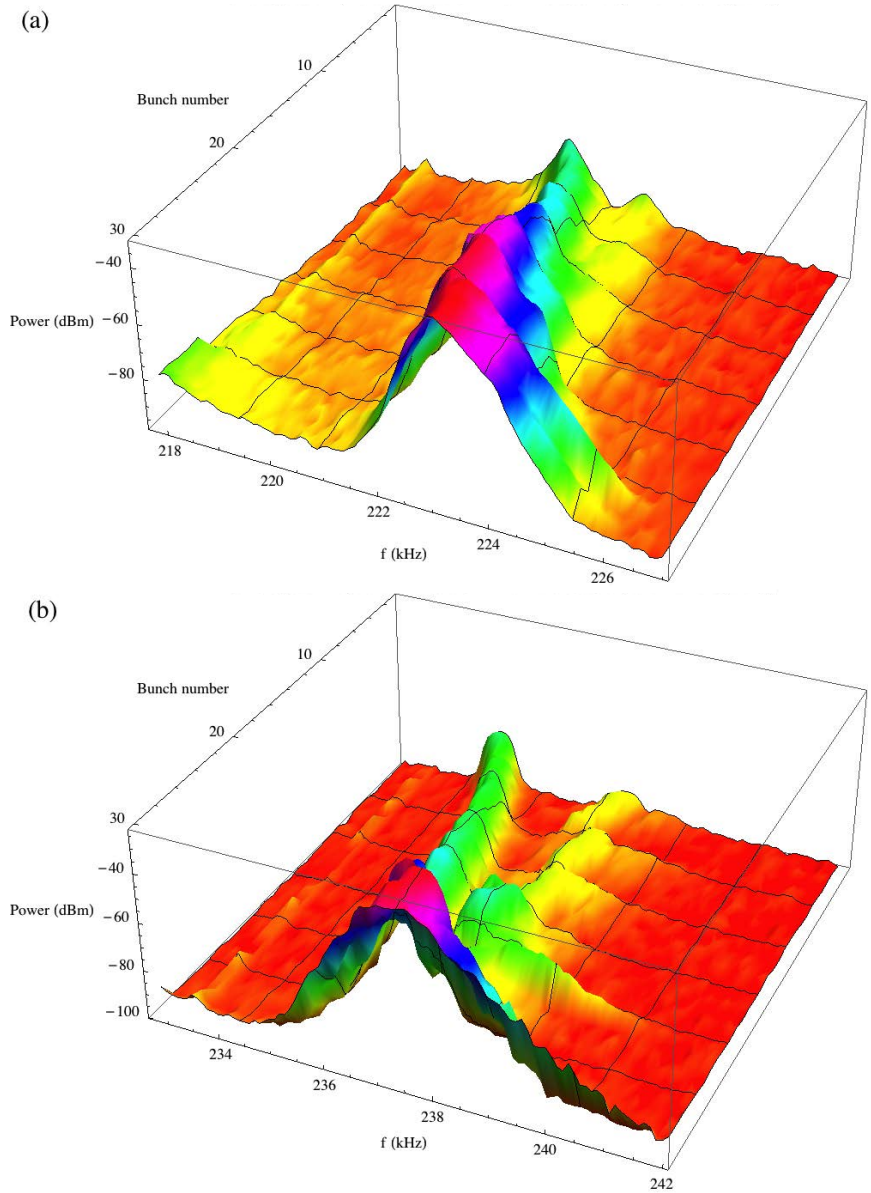

Figure 5. Bunch-by-bunch power spectra for the vertical betatron line for bunches of 0.75 mA currents in 30 bunch trains with (a) 14 ns bunch spacing (data set 166) and (b) 8 ns bunch spacing (data set 964).

3.2.3 Horizontal and Vertical Betatron Lines: Peak Power and Frequency

The relative signal power of the horizontal and vertical betatron lines is determined in the following manner: A 10 kHz wide frequency region is selected, centered approximately on the frequency of interest and the spectrum is fit to a single or, in the case when splitting of power spectrum occurs, a double Gaussian distribution to determine the background power level, width, amplitude, and frequency of the betatron line in this region. Then the maximum value of the power (the Gaussian distribution's amplitude) in this region is found and the background power level is subtracted from the peak power level to obtain the relative power (Fig. **??**). Because the background is subtracted,

if the relative power is close to zero (as we will see later in this paper in the plots of head-tail line power), this signifies the absence of any significant peak in the spectrum in the region selected. The frequency plots present the center frequency for the power spectrum peaks. The errors shown in the frequency plots correspond to the bin widths of the frequency spectra (100 Hz). The errors shown in the relative power plots are estimated from the variation in the power over a spectral bin width. In Fig. **??** the frequency of the spectral peak is given relative to the frequency of the first bunch. Thus Fig. **??** illustrates the tune shift along the train, which is primarily due to the electron cloud effect. The horizontal and vertical betatron tune shift along the bunch train is measured with respect to the first bunch of the train and has been found to be dependent on a number of parameters, such as bunch spacing and bunch current. From Fig. **??** several observations of the tune shift are:

- The vertical and horizontal tune shift is dependent on bunch spacing and bunch current. When the bunch spacing is increased the tune shifts decrease along the bunch train. As the bunch current increases, the tune shifts increase along the bunch train.
- Independent of bunch spacing, the horizontal tune is small until bunch 13 in a 30 bunch train. After bunch 13 the horizontal tune shift is nonlinear and has a strong dependence on bunch spacing.
- The vertical tune shift along the bunch train is visible roughly from the begining of the bunch train and increases linearly along the train.
- Most data jumps in the tune shift are caused when the current in the train is refilled. As an example the jump in the horizontal tune shift after bunch 25 is due to the current refilled before measuring bunch 26.

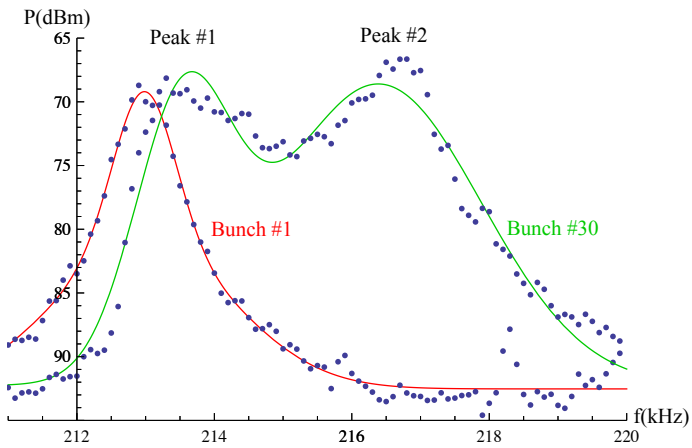

Figure 6. The power spectrum of bunch 1 and bunch 30 of a 30 bunch train that is centered at the horizontal betatron line fit to a double Gaussian distribution to determine the frequency, amplitude, and width of the betatron line in this window.

3.3 Cloud Density from Measured Betatron Tune Shifts

In this section the measured tune shifts are used to estimate the average electron cloud density. For a lattice in which the average beta functions are equal in both planes, the electron-cloud-induced

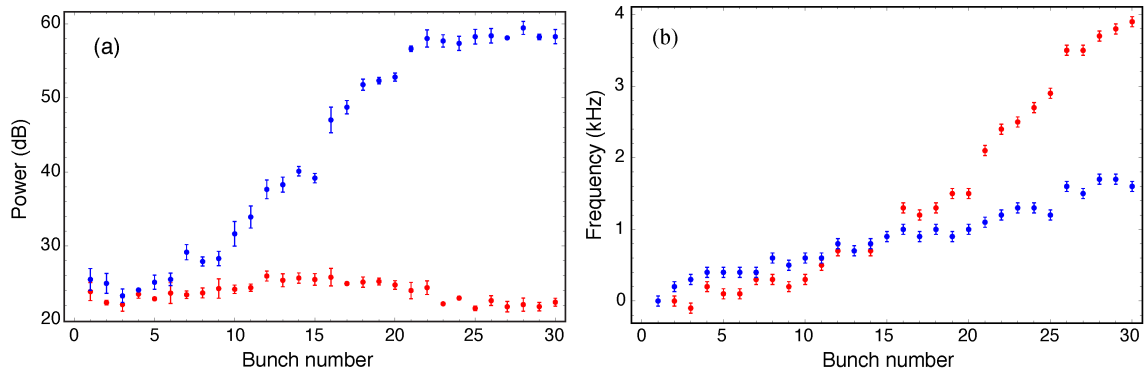

Figure 7. (a) Power of the horizontal and vertical spectral peaks as a function of bunch number; (b) Horizontal and vertical tune shifts as a function of bunch number for 30 bunch train of positrons with 14 ns bunch spacing. Chromaticity: (H,V) = (1.33, 1.16). Bunch current = 0.74 mA.

tune shifts δQ_x and δQ_y may be directly related to the average electron cloud density $\langle \rho_c \rangle$ via the relation [?]

$$\langle \rho_c \rangle = \gamma \frac{\delta Q_x + \delta Q_y}{r_e \langle \beta \rangle C}, \tag{3.1}$$

in which $\langle \beta \rangle$ is the average beta function, C is the ring circumference, γ is the beam Lorentz factor and r_e is the classical electron radius. This relation may be used to obtain an estimate of the cloud density along the train. For CesrTA we use $C = 649$ m (sum of all drift and dipole lengths) and $\langle \beta \rangle = 16$ m. The cloud densities for each bunch resulting from this calculation is shown as a function of bunch spacing in Fig. **??** and as a function of bunch currents in Fig. **??**. We can conclude from the electron cloud density plots (Fig. **??** and Fig. **??**) that:

- The electron cloud density increases as the bunch spacing decreases. Along the bunch train it goes from a rather linear increase with bunch number (for 14-28ns bunch spacing) to a non-linear dependence (for 4-12ns bunch spacing).
- The electron cloud density is highly dependent on bunch current. As the current increases there is a change in the slope of the electron cloud density for closely spaced bunches. The transition in the slope occurs around bunch 13.

3.4 Vertical Head-tail Lines

3.4.1 Head-tail Line Power and Frequency Characteristics

As shown in Fig. **??** and Fig. **??** there are two lines, which appear in the bunch-by-bunch power spectrum starting part way along the train and have frequencies close to the betatron frequency plus and minus the synchrotron frequency. A detailed view of the bunch-by-bunch power spectrum located at $Q_y - Q_s$ is shown in Fig. **??** for two different vertical chromaticites.

The power and frequency of the head-tail lines, $Q_y \pm Q_s$, are determined in the same manner as the horizontal and vertical betatron lines except the spectrum is only fit to a single Gaussian distribution to determine the background power level, width, amplitude, and frequency of the head-tail line (Fig. **??**). Several interesting features of this analysis are evident in Fig. **??**:

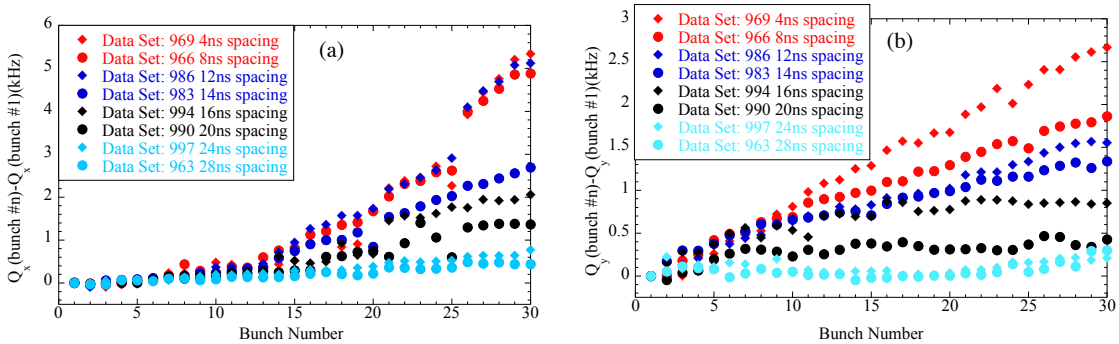

Figure 8. (a) Horizontal and (b) vertical betatron tune shift along a 30 bunch train for bunch spacings between 4-28ns. Bunch current = 0.75 mA.

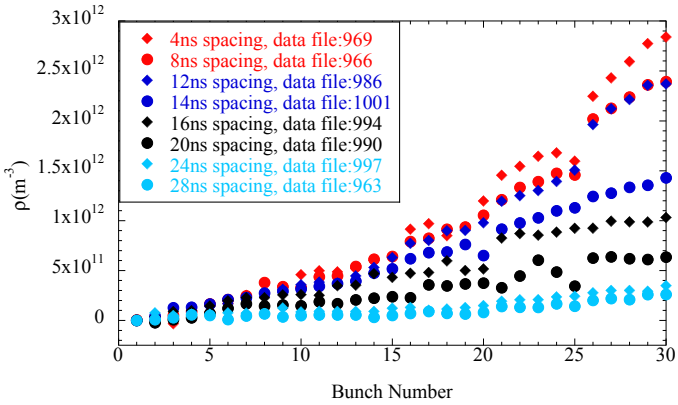

Figure 9. Average electron cloud density for bunch spacings between 4-28ns at E=2.085Gev for bunch current of 0.75mA.

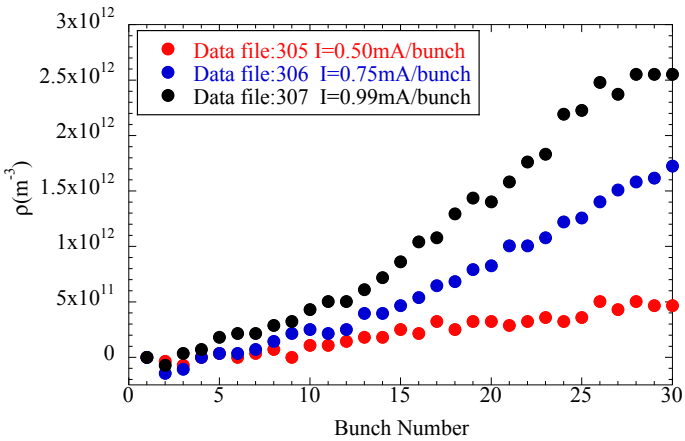

Figure 10. Average electron cloud density along a 30 bunch train for different bunch currents. All of the data is at 2.085 GeV beam energy.

- When the vertical chomaticity is increased the vertical head-tail line signal, power, shape, and width, decreases.

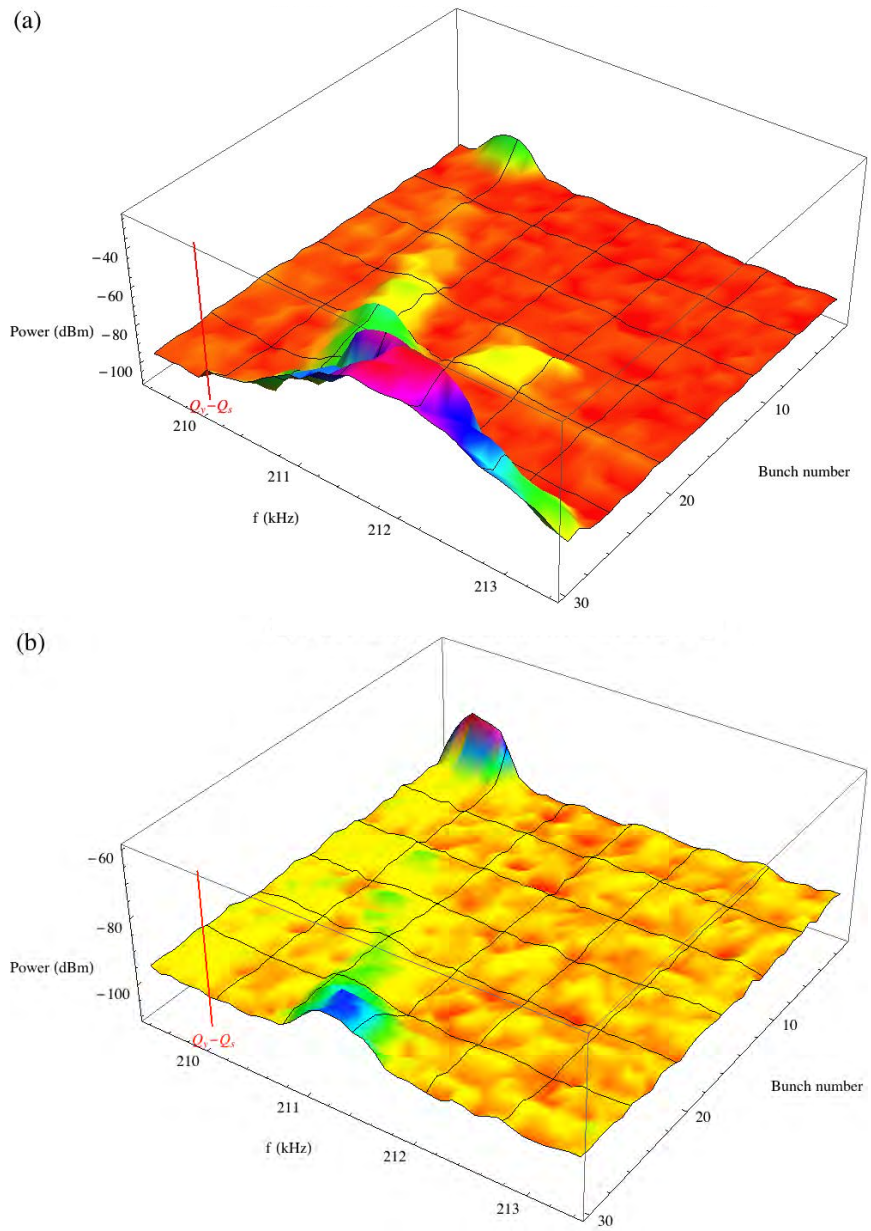

Figure 11. $Q_y - Q_s$ vertical head tail lines for 30 bunch train with 8 ns bunch spacing with the following beam parmeters: (a) Chromaticity: (H,V) = (-1.17,-1.07) and bunch current = 0.74 mA (Data set 964). (b) Chromaticity: (H,V) = (-1.18,-0.89) and bunch current = 0.74 mA (Data set 966).

- The vertical head-tail line shift in frequency correlates with the shift in frequency of the vertical betatron line.
- For close bunch spacings, typically 4-12 ns bunch spacings, the head-tail line is observed at the start of the train but then disappears until the end of the train. Adding a precursor bunch, a bunch just before the start of the train, will make the signal at the start of the train disappear.

In Fig. **??**a, we plot the power (relative to the vertical betatron line) and the frequency (± the

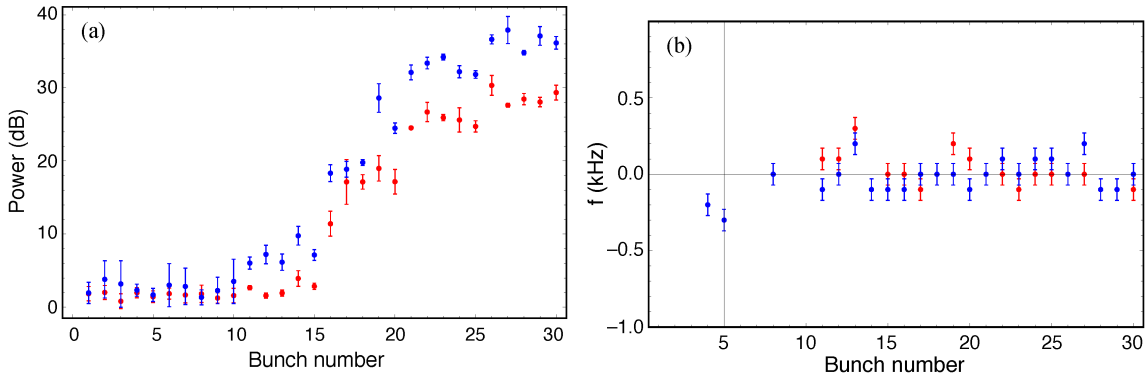

Figure 12. Vertical head tail lines: (a) peak power vs. bunch number, and (b) the frequency difference from vertical betatron line vs. bunch number, were the synchrotron frequency is added/subtracted from the offset. Chromaticity: (H,V) = (1.33, 1.16). Bunch current = 0.74 mA.

synchrotron frequency) of these lines. We associate the lower frequency line with the $m = -1$ head-tail line, which arises as a result of head-tail bunch motion driven by the broadband impedance of the electron cloud. Similarly, we associate the higher frequency line with the $m = +1$ head-tail line. From Fig. **??**a, we see that these lines appear above the noise level around bunch 15 or 16. The $m = -1$ line is somewhat more strongly excited than the $m = +1$ line. Similar measurments of the head-tail lines have been made at the B-factory at the High Energy Accelerator Research Organisation (KEK) in Tsukuba, Ibaraki Prefecture, Japan [**?**]-[**?**].

Observations of beam size growth under similar beam conditions (see Section **??**) show rapid emittance growth starting at about the same point in the train

For this particular data set Fig. **??**b shows that for bunch numbers greater than about 15, where the head-tail lines appear above the background, the frequency difference between these head-tail lines and the vertical betatron line is equal to the synchrotron frequency (within the errors).

3.4.2 Head-tail Lines: Correlation with Cloud Density

Comparing Fig. **??** and Fig. **??**, the average electron cloud density, at which the head-tail lines are first observed, can be established. For the conditions shown in Fig. **??** (data set 166), the head-tail lines emerge at an average beam cloud density around 4×10^{11} m^{-3}.

3.4.3 Reproducibility

The reproducibility of the observations of the head-tail lines is illustrated in Fig. **??**. This plot shows the power in the vertical head-tail lines for three data sets taken on different dates (data set 147 on September 25, 2010, data set 157 on September 26, 2010, and data set 166 on September 28, 2010) but under the same nominal machine and beam conditions. Fig. **??** shows that the head-tail line observations are reasonably reproducible when the machine is set to the same nominal conditions.

3.4.4 Chromaticity Dependence

The chromaticity dependence of the head-tail lines is illustrated in Fig. **??**. For all data sets the nominal bunch current was abut 0.74 mA. We see that for data set 142, with a higher value of

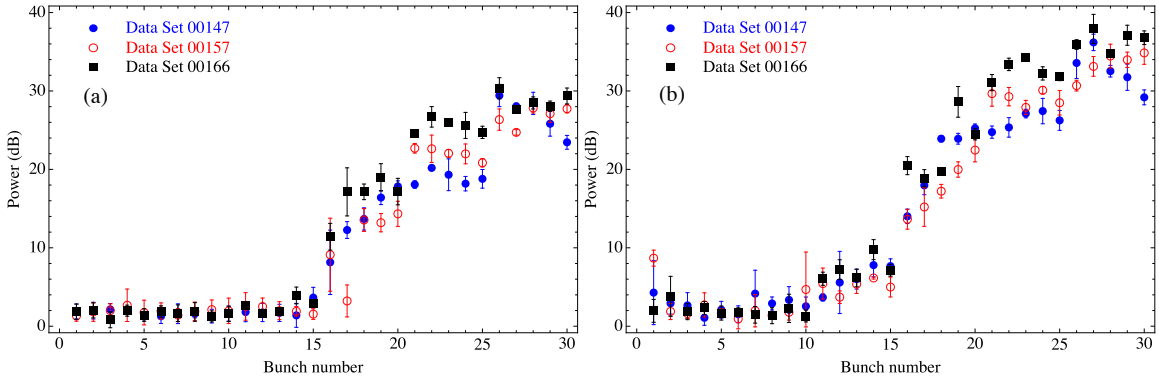

Figure 13. Comparison of vertical head-tail lines for (a) m=1 and (b) m=-1 when all three data sets have the same nominal bunch current (about 0.74 mA), 14 ns bunch spacing, and chromaticity (H,V)=(1.33, 1.16).

the vertical chromaticity than data set 147, there are no head-tail lines observed. For data set 129 with lower values of both chromaticities than data set 142, head-tail lines are observed, but their excitation levels are lower than in data set 147, which has the lowest vertical chromaticity.

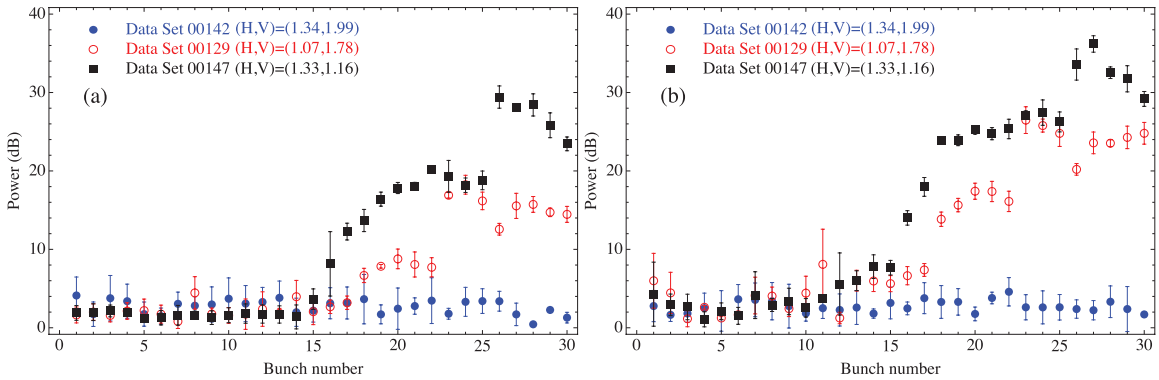

Figure 14. Comparison of vertical head-tail lines for (a) m=1, and (b) m=-1 for three different data set with the same nominal bunch current (about 0.75 mA) but different chromaticities, as follows 142: (H,V) = (1.34, 1.99); 129: (H,V) = (1.07, 1.78); 147: (H,V) = (1.33, 1.16)

3.4.5 Current Dependence

The current dependence of the head-tail lines is illustrated in Fig. **??** and Fig. **??**. In Fig. **??** both data sets have the same chromaticity, but the data set with the lower bunch current (data set 142) shows no head-tail lines, while the higher current data set (data set 150) shows head-tail lines starting to emerge around bunch 12. Similarly in Fig. **??** both data sets have the same (lower) chromaticity, but the data set with the lower bunch current (data set 178) shows no head-tail lines, while the higher current data set (data set 147) shows head-tail lines staring to emerge around bunch 13. From Fig. **??** and Fig. **??** it is evident that the m=-1 head-tail line appears earlier in the bunch train than the m=+1 head tail line.

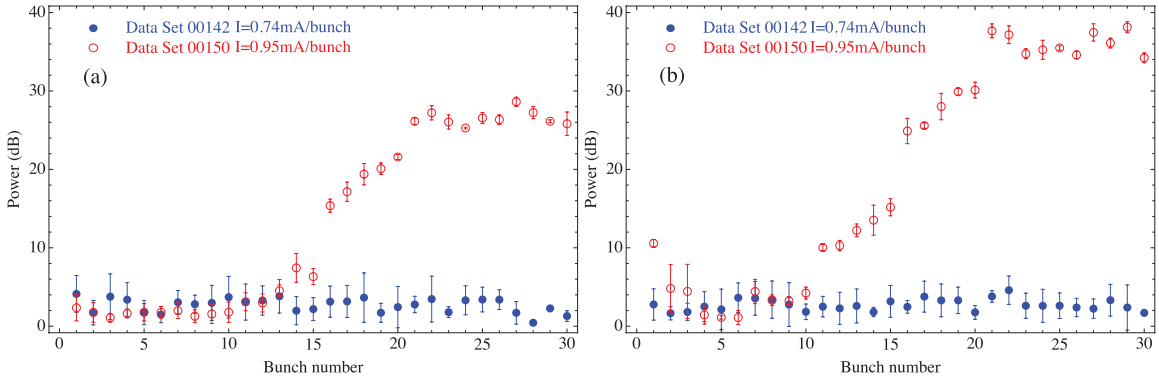

Figure 15. Comparison of vertical head-tail lines from 30 bunch train with 14 ns bunch spacing for (a) m=1 and (b) m=-1 for two data sets with the same chromaticity [(H,V) = (1.34, 1.99)] but different bunch currents as follows: 142: 0.74 mA; 150: 0.95 mA

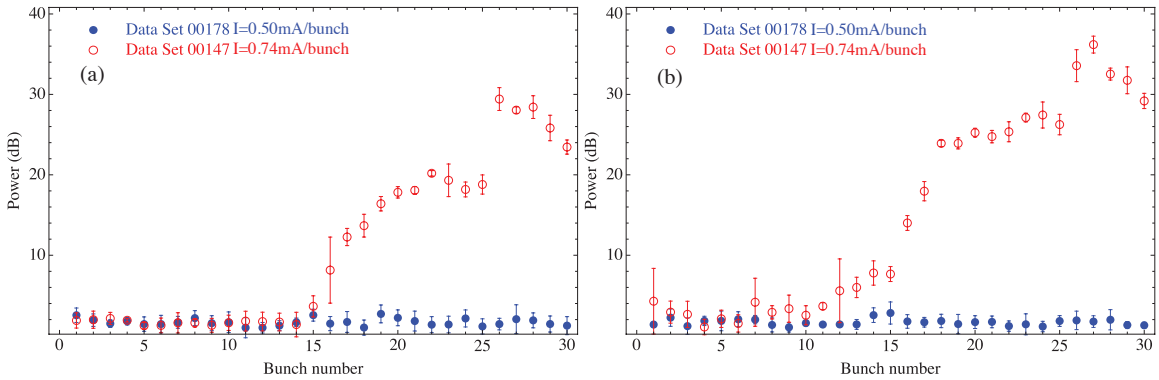

Figure 16. Comparison of vertical head-tail from 30 bunch train with 14 ns bunch spacing lines for (a) m=1 and (b) m=-1 for two data sets with the same chromaticity [(H,V) = (1.33, 1.16)] but different bunch currents as follows: 147: 0.74 mA; 178: 0.5 mA

3.4.6 Bunch Number Dependence

The bunch number dependence of the head-tail lines is illustrated in Fig. **??**. Both data sets have the same chromaticity and bunch current, but one contains 45 bunches in the train (data set 156). The vertical tunes of the first bunch were slightly different for the two runs: for run 142, it was about 227 kHz, while for run 156 the tune was about 221 kHz. No head-tail lines are observed in data set 142 out to the end of the train, bunch 30. But with 45 bunches, head-tail lines are observed starting around bunch 18, then growing to a peak around bunch 25, and falling off at the end of the train. The fact that the head-tail lines are seen with a 45 bunch train with the same bunch current as a 30 bunch train, for which no lines are seen, is suggestive that there is a residual cloud density which lasts more than one turn and which depends on the total current.

3.4.7 45 Bunch Train: Correlation with Cloud Density

In Fig. **??** we show the cloud density as a function of bunch number, computed from the measured tune shifts discussed above and using equation (1). Comparison with Fig. **??** shows that the head-tail lines emerge from the background at a cloud density of about 4×10^{11} m^{-3}, which is the same

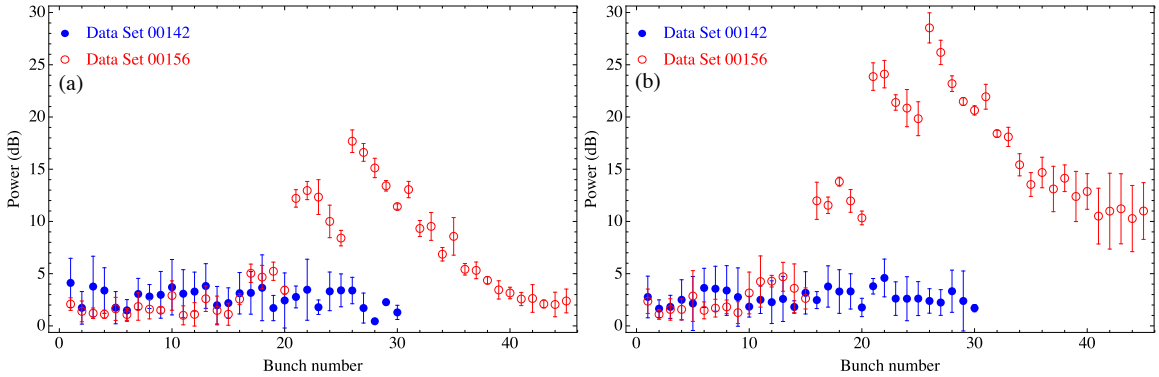

Figure 17. Comparison of vertical head-tail lines for (a) m=1 and (b) m=-1 for 30 and 45 bunch trains. Both trains have the same chromaticity [(H,V) = (1.34, 1.99)] and bunch current (0.74 mA). The increased amplitude for the 45 bunch train at bunches 21 and 26 is an artifact due to refilling of the train at these bunch numbers.

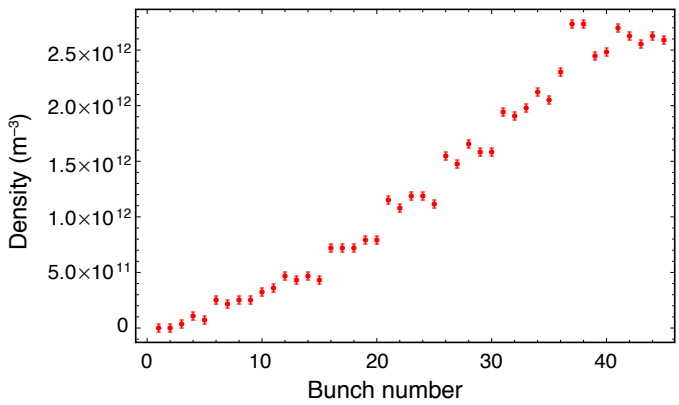

Figure 18. Electron cloud density vs. bunch number for a 45 bunch train with 14 ns spacing and bunch current of 0.74 mA/bunch.

as the threshold density found for data set 166, even though the vertical chromaticity was higher for data set 156. The fall-off of the head-tail lines after bunch 25 suggests that the instability is saturating. Yet the cloud density continues to increase after bunch 25 (at least until around bunch 35) as Fig. **??** shows. The head-tail instability threshold is expected to be sensitive to the vertical beam size. What may be happening is that the instability is driving vertical beam size growth along the train and the increase in the threshold as the beam size increases provides a mechanism for the instability to saturate.

3.4.8 Synchrotron Tune Dependence

The synchrotron tune dependence of the head-tail lines is illustrated in Fig. **??**. Both data sets have the same chromaticity and bunch current, but data set 151 has a reduced synchrotron frequency of 20.7 kHz and a larger bunch length of 12.8 mm. For data set 147 the nominal frequency and bunch length are 25.4 kHz and 10.8 mm, respectively.

For both data sets, the separation between the vertical betatron lines and the head-tail lines

equals the synchrotron frequency. Fig. **??** shows that the head-tail line threshold is about the same in both cases, but the power in the lines grows more slowly with bunch number for the data set with a reduced synchrotron frequency (i.e. a longer bunch length).

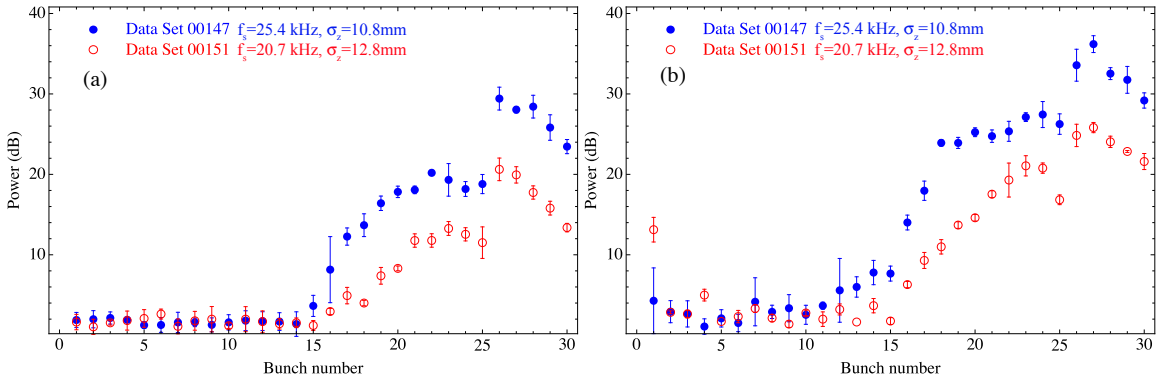

Figure 19. Comparison of vertical head-tail lines for (a) m=1 and (b) m=-1 with both data sets have the same chromaticity [(H,V) = (1.33, 1.16)] and bunch current (0.74 mA), but different values of the bunch length and synchrotron frequency, as follows: 147, f_s = 25.4 kHz and σ_z = 10.8 mm; 151, f_s = 20.7 kHz and σ_z = 12.8 mm.

3.4.9 Single-bunch Vertical Emittance Dependence

The vertical emittance dependence of the head-tail lines is illustrated in Fig. **??**. Both data sets have the same chromaticity and bunch current, but data set 158 has an increased single-bunch vertical emittance of approximately 300 pm [1]. The nominal single-bunch vertical emittance, for data set 147, is approximately 20 pm.

Fig. **??** shows that the head-tail line growth is very similar for the two different vertical emittances. The power in the lines seems to plateau at a lower level for the data set with smaller vertical emittance. Generally, there is not a great deal of difference visible in the data.

Another observation which explores the vertical emittance dependence of the head-tail lines is shown in Fig. **??**. Both data sets have 45 bunches and have the same chromaticity and bunch current, but data set 159 has an increased single-bunch vertical emittance of approximately 300 pm. The single-bunch vertical emittance, for data set 156 is approximately 20 pm.

Inspecting Fig. **??** we see that, in this case, the power in the lines peaks at a lower level and at a later bunch for the data set with smaller vertical emittance. This would suggest that the instability is slightly stronger for the case of larger vertical emittance. In addition the power in the lines for the large vertical emittance jumps when the bunch train current is topped off which demonstates the instabilities sensativity to bunch current.

3.4.10 Vertical Feedback Dependence

The vertical feedback dependence of the head-tail lines is illustrated in Fig. **??**. Both data sets have the same chromaticity and bunch current, but data set 126 has the vertical (dipole) feedback off.

[1]This number was estimated from a lattice model, not directly measured.

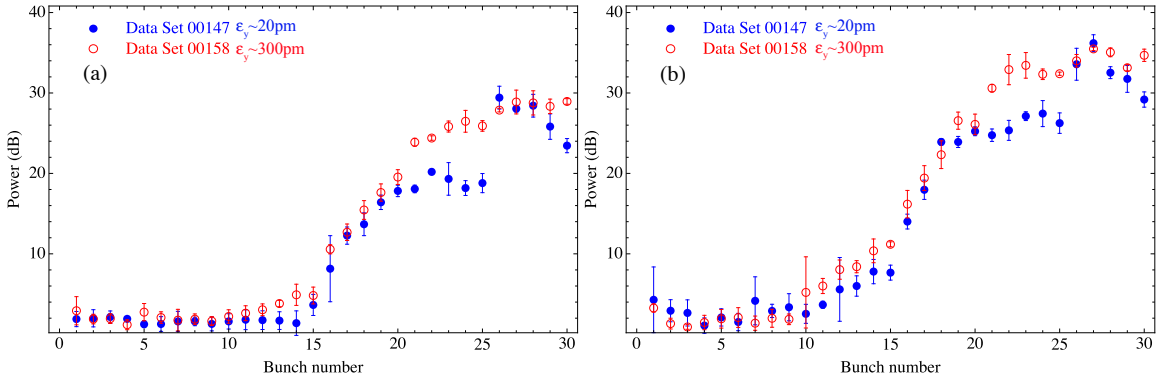

Figure 20. Comparison of vertical head-tail lines for (a) m=1 and (b) m=-1 with both data sets have the same chromaticity [(H,V) = (1.33, 1.16)] and bunch current (0.74 mA), but different values of the single-bunch vertical emittance, as follows: 147, Vertical emittance approximately 20 pm; 158, Vertical emittance approximately 300 pm

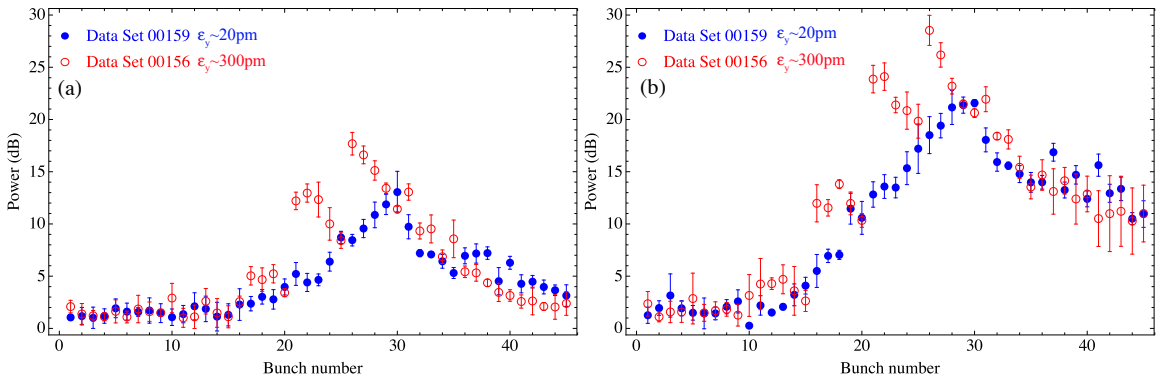

Figure 21. Comparison of vertical head-tail lines for (a) m=1 and (b) m=-1 with both data sets have 45 bunches, the same chromaticity [(H,V) = (1.34, 1.99)] and bunch current (0.74 mA), but different values of the single-bunch vertical emittance, as follows: 156, Vertical emittance ~ 20 pm; 159, Vertical emittance ~ 300 pm

For data set 129, as for all the other data sets discussed here (except 126), the vertical feedback is set to 20% of full gain.

Fig. **??** shows that the head-tail line threshold is about in the same place for these two data sets. But for data set 126 (feedback off) the power peaks a few dB higher than for data set 126 and then falls off.

3.4.11 Beam Energy Dependence

In data set 265 the structure of the frequency spectrum was studied for a beam energy of 4 GeV. Fig. **??** shows the beam current as a function of bunch number for this data set. The bunch current was about 1.1 mA/bunch and the beam lifetime at the higher energy is much better than at lower energy. The machine parameters for this measurement are presented in Table **??**

Power Spectrum Fig. **??** shows the power spectrum as a function of bunch number. Clearly visible are the horizontal and vertical betatron lines, the head-tail line above the vertical, and another

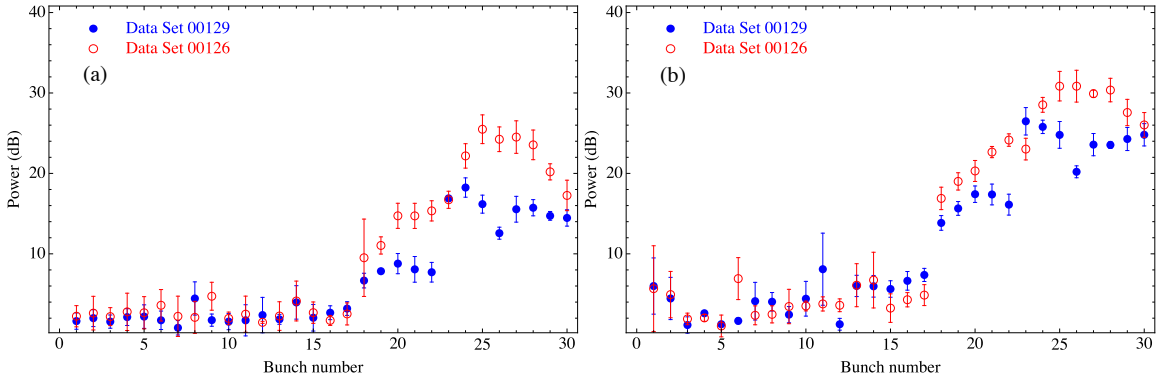

Figure 22. Comparison of vertical head-tail lines for (a) m=1 and (b) m=-1 with both data sets have the same chromaticity and bunch current, but different values of the vertical feedback, as follows: 126, Vertical feedback off; 129, Vertical feedback at 20% of full gain.

line around 285 kHz. The line at 285 kHz corresponds to excitation of the $Q_x + 2Q_y = 2$ resonance.

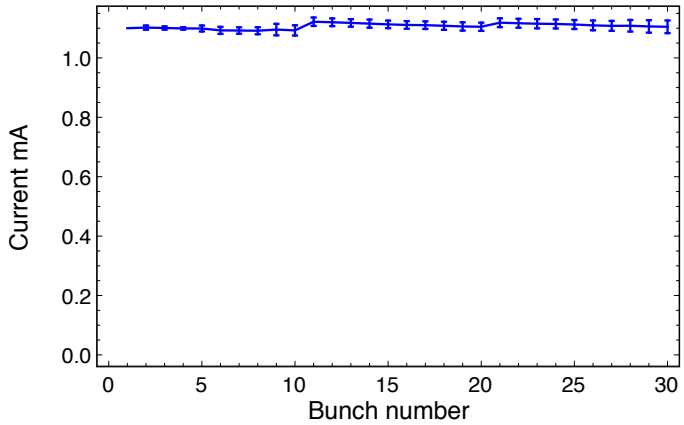

Figure 23. Bunch-by-bunch currents, 4 GeV beam energy

Betatron Lineshapes Fig. **??** shows the bunch-by-bunch power spectrum near the horizontal betatron line. As at 2 GeV, there is a major peak, which shifts up in frequency approximately 4 kHz during the bunch train. This shift is attributable to the electron cloud. Fig. **??** shows the bunch-by-bunch power spectrum near the vertical betatron line. There is considerably more structure in this line than at 2 GeV, including a splitting of the main peak which persists throughout the train, and some smaller satellite peaks which seem to develop after bunch 20.

Vertical Head-tail Lines In Fig. **??**a we plot the power (relative to the noise floor) and the frequency (± the synchrotron frequency) in Fig. **??**b of the head-tail lines. We see that these lines appear above the noise level around bunch 18. The lower frequency line ($m = -1$ head-tail line) is close to the horizontal line, and is weakly excited so its power is not well determined and is omitted from the frequency plot. The frequency plot shows that for the ($m = +1$ head-tail line) the head-tail line frequency minus the vertical betatron line frequency differs from the synchrotron frequency

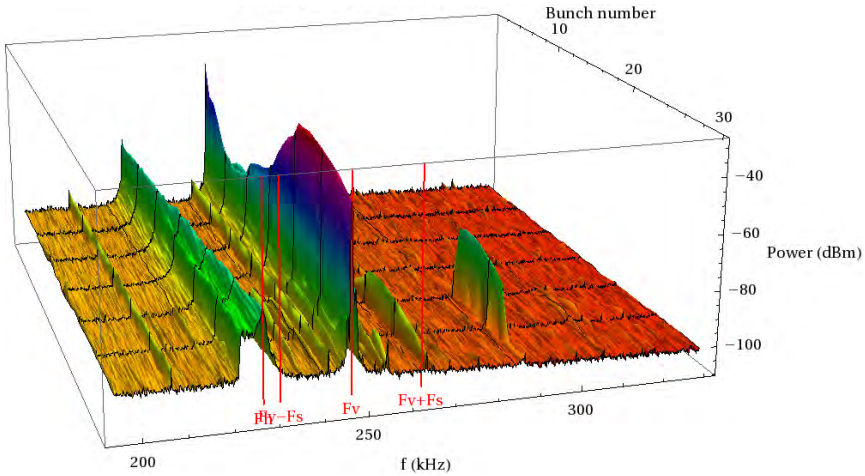

Figure 24. Bunch-by-bunch power spectrum for 30 bunch train at 4 GeV with chromaticity of: (H,V) = (1.3, 1.4), and bunch current of 1.1 mA.

Table 2. Nominal machine parameters at 4 GeV. The emittances and tunes are those of a single bunch in the storage ring.

Parameter	**Value**	**Unit**
Energy	4.00	GeV
Lattice	4000 mev_23 nm_20090816	
Horizontal emittance	23	nm
Vertical emittance	~ 180	pm
Bunch length	17.2	mm
Horizontal tune	14.55	
Vertical tune	9.58	
Synchrotron tune	0.041	
Momentum compaction	6.3×10^{-3}	
Revolution frequency	390.13	kHz

by about 1 kHz. This is in contrast to the observations made at 2 GeV, for which this difference is essentially zero.

Instability Threshold Estimate In Fig. **??**, we show the cloud density as a function of bunch number, computed from the measured tune shifts, as discussed above. Comparison with Fig. **??**a shows that the head-tail lines emerge from the background at a cloud density of about 1.2×10^{12} m^{-3}.

3.4.12 Beam Particle Species Dependence

The beam species (e^+ or e^-) dependence of the bunch-by-bunch power spectrum is illustrated by comparing data set 166 (Fig. **??**) and data set 154 (Fig. **??**). Both data sets have the same chromaticity and bunch current, but data set 154 is for an electron beam. In this latter case we

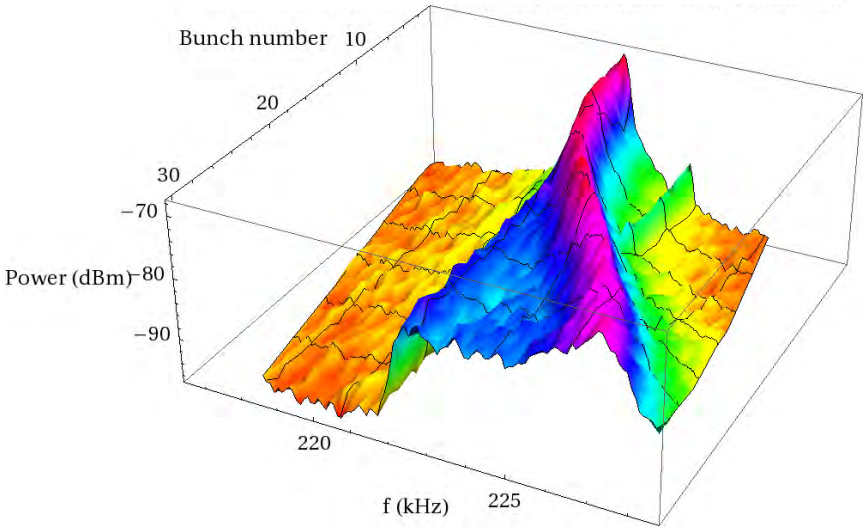

Figure 25. Bunch-by-bunch power spectrum at horizontal betatron line for 30 bunch train at 4 GeV. Chromaticity: (H,V) = (1.3, 1.4). Bunch current = 1.1 mA.

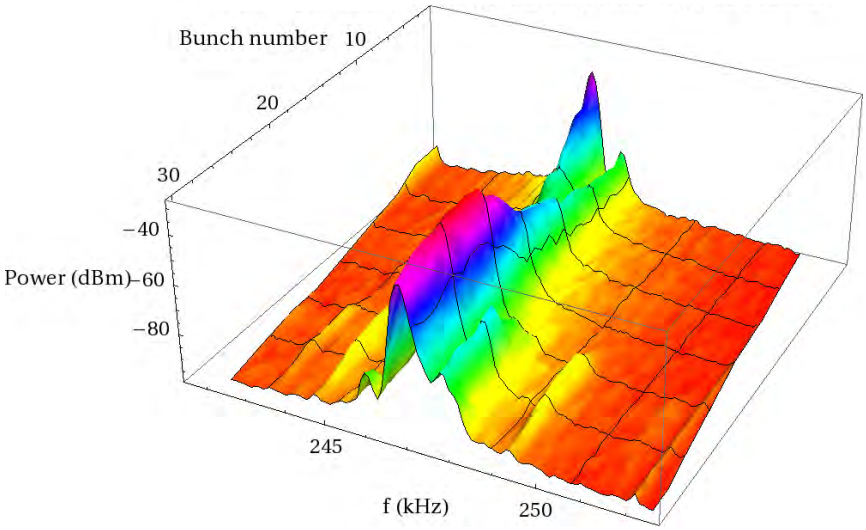

Figure 26. Bunch-by-bunch power spectrum at vertical betatron line for 30 bunch train at 4 GeV. Chromaticity: (H,V) = (1.3, 1.4). Bunch current = 1.1 mA.

see less vertical excitation along the train, and smaller head-tail line excitation, than for a positron beam. The large tune shifts observed with the positron beam are also absent. The details of the different structures of the head-tail lines for electrons and positrons can be seen in Fig. **??**. For electrons the head-tail lines start later in the train, grow slowly, and at their maxima are 20 dB lower than the positron head-tail lines.

The positron-beam head-tail excitation is presumably due to electron cloud effects. The physical mechanism responsible for the head-tail excitation in the electron case is not likely a result of the electron cloud but possibly due to positive ions or wakefield effects.

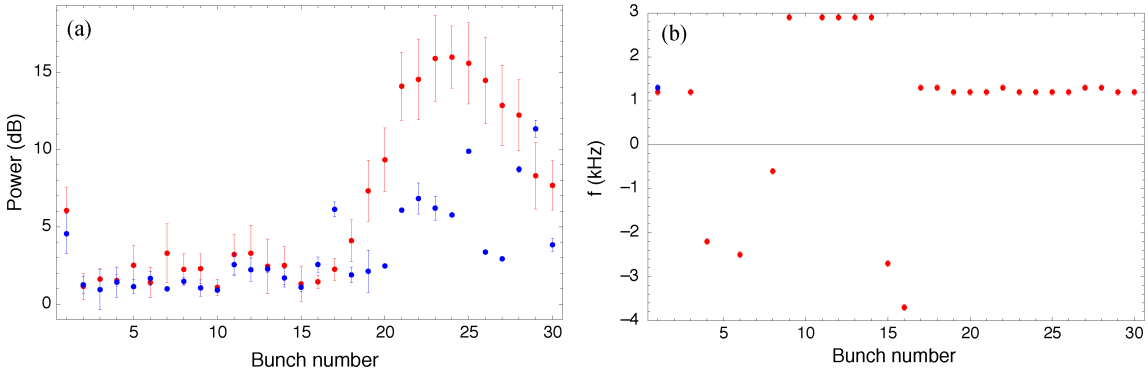

Figure 27. Vertical head tail lines: (a) peak power vs. bunch number; (b) frequency difference from vertical betatron line vs bunch number, with the synchrotron frequency removed from the offset. Beam energy 4 GeV. Chromaticity: (H,V) = (1.3, 1.4). Bunch current = 1.1 mA.

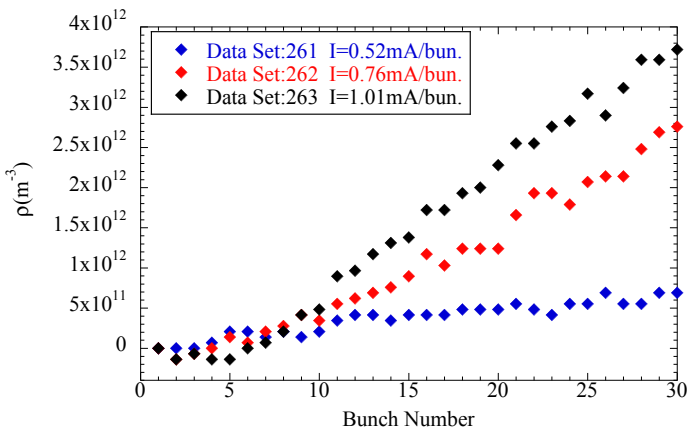

Figure 28. Electron cloud density along a 30 bunch train at three different bunch currents for a 4 GeV beam energy.

3.4.13 Precursor Bunch Dependence

At 2 GeV in Fig. **??** the power spectrum of bunch 1 for data set 151 is shown (red trace). Note the presence of a prominent $m = -1$ head-tail line. This line disappears for the second bunch and does not re-appear until much later in the train, as shown in Fig. **??**. Moreover beam size measurements (see Section **??**) indicate that the first bunch in the train is frequently larger in size than the next few bunches.

This suggests that the trapped cloud density near the beam, which persists after the train ends, may be sufficiently high even for the first bunch in the train that spontaneous head-tail motion occurs. However, the interaction of the first bunch with this trapped cloud evidently destabilizes it, causing it to disperse, so that bunch 2 does not suffer from spontaneous head-tail motion.

Simulations and witness bunch measurements indicate that the electron cloud lifetime in dipoles and drifts is much shorter than one turn in CesrTA. Electron clouds which persists for many turns may be due to trapped cloud in quadrupoles or wigglers. Simulations and retarding field analyzers (RFAs) measurements in quadrupoles have both indicated that trapped cloud may be present [**?**].

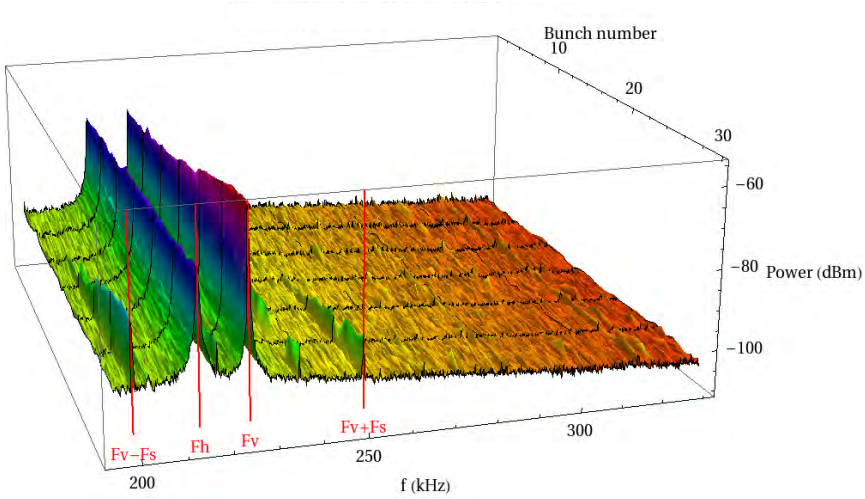

Figure 29. Bunch-by-bunch power spectrum of a 30 bunch electron beam with the same chromaticity and bunch current parameters as the 30 bunch positron beam shown in Fig. **??**.

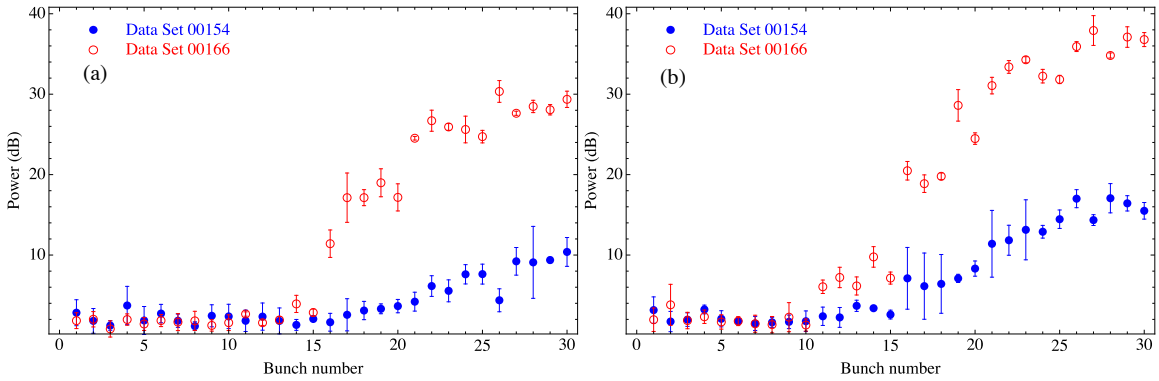

Figure 30. Vertical head-tail lines for (a) m=1 and (b) m=-1 for data sets that have the same chromaticity and bunch current for a 30 bunch train of positrons (166) and electrons (154).

To test this hypothesis (in data set 153) a 0.75 mA "precursor" bunch was placed 182 ns before bunch 1. Otherwise, conditions were the same as for data set 151. The spectrum of the first bunch for data set 153 is shown (blue trace) in Fig. **??**. Note that the lower head-tail line is now absent. In addition the structure seen on the upper edge of the vertical betatron line in Fig. **??** also disappears. Finally, there is a small line at 235.7 kHz (13.6 kHz above the vertical betatron line), which also disappears when the precursor bunch is introduced.

It is quite interesting to note that the frequency difference between the head-tail line of the first bunch for data set 151 (shown in Fig. **??**) and the vertical betatron line is 20.2 $\pm$ 0.1 kHz, which is significantly different from the synchrotron frequency, 20.7 kHz. At 2 GeV the head-tail lines, which develop later in the train both above and below the vertical betatron line, always have a separation equal to the synchrotron frequency within the measurement errors (see Fig. **??**).

We have observed a prominent $m = -1$ head-tail line for the first bunch in the train in two other data sets: data set 150 (see Fig. **??**) and data set 157 (see Fig. **??**). In both of these cases the $m = -1$ line is separated from the vertical betatron line by significantly less (typically 0.6 to

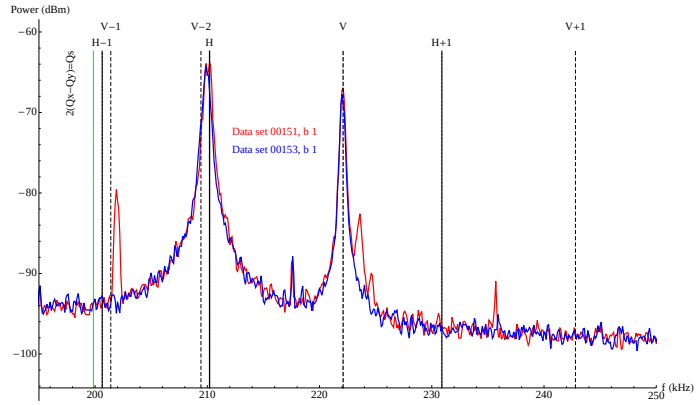

Figure 31. The power spectrum for two different data sets of bunch 1 with the same chromaticity and bunch current, but for one data set (153) a precursor bunch present, as described in the text. The lines labelled, for example,"V+1" and "V-1" are shown at frequencies of $\pm f_s$ from the vertical betatron line ("V"), in which f_s is the synchrotron frequency. For these data sets, $f_s = 20.7$ kHz. The location of a machine resonance is also indicated.

0.7 kHz) than the synchrotron frequency, and there is a doublet structure to the vertical betatron line as shown in Fig. **??** for data set 151.

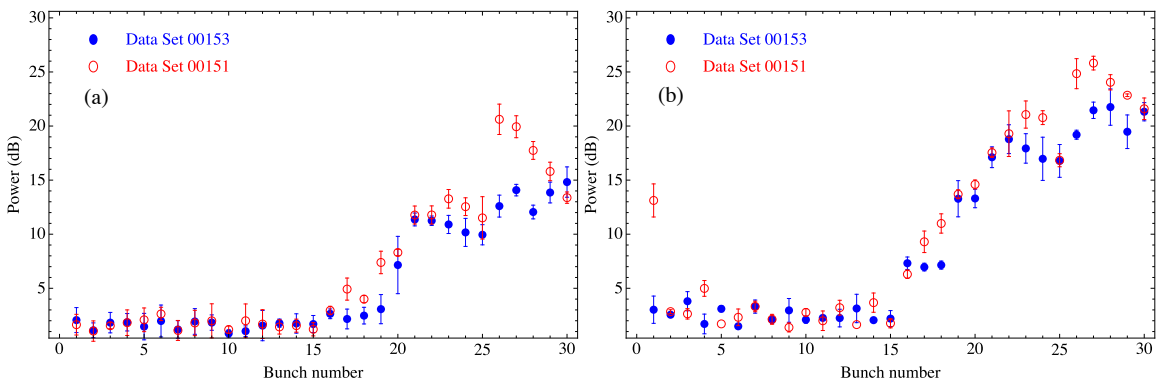

Figure 32. Comparison of vertical head-tail lines where both data sets have the same chromaticity and bunch current, but a precursor bunch is present for one of the data set (153), as described in the text.

In Fig. **??** the power in the vertical head-tail lines is shown as a function of bunch number for data sets 151 and 153. After the first bunch the figure shows little difference between the head-tail line growth for the two data sets. The data set without the precursor bunch has a slightly higher line power near the end of the train.

3.5 Single Bunch Current Variation Experiment

To explore further the dynamics of the interaction of the last bunch in the train with the cloud, a series of power spectral measurements were made, in which the current in the first 29 bunches in a 30 bunch train was fixed, but the current in the last bunch was varied. The power spectrum with the last bunch at 0.25 mA (data set 167) is compared with the power spectrum with the last bunch at 1.25 mA (data set 171) in Fig. **??**.

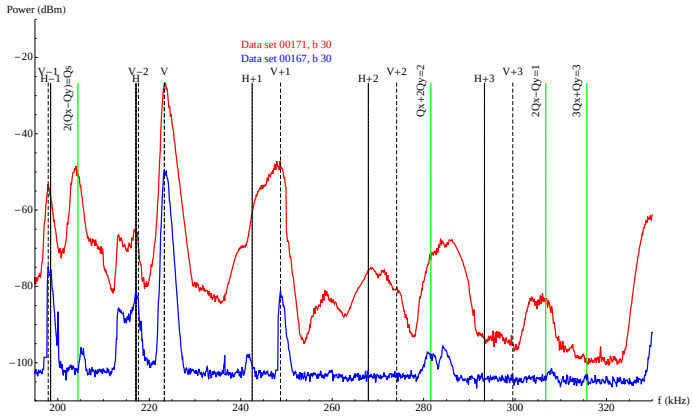

Figure 33. Data set 167 and data set 171: Comparison of the power spectra for bunch 30. The lines labeled "V+1" and "V-1" are shown at frequencies of $\pm f_s$ from the vertical betatron line ("V") in which f_s is the synchrotron frequency. The locations of several machine resonances are also indicated. The first 29 bunches had a nominal current of 0.75 mA/bunch. Chromaticity: (H,V) = (1.33, 1.16). For data set 167, bunch 30 had a current of 0.25 mA. For data set 171, bunch 30 had a current of 1.25 mA.

The vertical excitation of the bunch, both at the vertical betatron line and at the head-tail lines, is somewhat larger than the expected 14 dB increase for the higher current bunch. The $m = +1$ head-tail line appears to acquire a low-frequency shoulder at the higher current.

In addition the frequency of the vertical betatron line is almost independent of the current in the bunch. The shift from 0.25 mA to 1.25 mA is less than 0.2 kHz. Note that this behavior is less than what would be expected for the machine impedance, for which one would expect -0.35 kHz tune shift for a 1 mA change in the bunch current.

3.6 Summary

The basic observation is that under a variety of conditions for some of the bunches within the train, the single-bunch frequency spectra of multi-bunch positron trains exhibit the $m = \pm 1$ head-tail (HT) lines, separated from the vertical line by the synchrotron frequency. A summary of more detailed observations is presented in the following list.

- For a 30 bunch train with 0.75 mA/bunch at 2.1 GeV beam energy, the onset of the HT lines occurs at a cloud density of around 4×10^{11} m^{-3} (assuming no cloud density at the start of the train).
- For a 30 bunch train with 1.1 mA/bunch at 4 GeV beam energy, the onset of the HT lines occurs at a cloud density of around 1.2×10^{12} m^{-3} (assuming no cloud density at the start of the train).
- The betatron lines exhibit structure which varies along the train. The vertical dipole mode power grows along the train and has a fine structure that is not understood.
- The amplitude of the HT lines depends strongly on the vertical chromaticity, the beam current and the number of bunches.

- For a 45 bunch train the HT lines have a maximum power around bunch 30; the spectral power is reduced for later bunches.
- There is a weak dependence of the onset of the HT lines on the synchrotron tune, the single-bunch vertical emittance and the vertical feedback.
- Under identical conditions HT lines also appear in electron-beam trains, but the onset is later in the train, develops more slowly and is much weaker than for positron beam trains.
- Under some conditions the first bunch in the train also exhibits a head-tail line ($m = -1$ only). The presence of a "precursor" bunch can eliminate the $m = -1$ signal in the first bunch. One conjecture is that there may be a significant "trapped" cloud density near the beam, which lasts long after the bunch train has ended and which is dispersed by the precursor bunch.
- There is a strong dependence of the HT line structure observed on last bunch in a 30 bunch train, as a function of the current in that bunch. But the frequency of the vertical betatron line of this bunch is only very weakly dependent on the current in the bunch.

4 Emittance Growth Along Bunch Trains: Experimental Studies

This section discusses measurements made using the x-ray beam size monitor (xBSM) that consists of a 32-linear pixel array. The xBSM can measure the vertical profile of each bunch turn-by-turn for multiple turns (e.g. 1024 or 4096 turns). A description of the xBSM is detailed elsewhere ([**?**] and [**?**]). All measurements were made in the 2 GeV low-emittance lattice unless otherwise noted.

4.1 Bunch Current Dependence

To quantify the vertical beam size growth along a bunch train measurements were made with the bunches at 14 ns spacing, using 30 and 45-bunch trains with feedback on [**?**]. For each bunch the turn-by-turn vertical sizes and positions were fitted and then the sizes were averaged over all turns (typical data sets are either 1024 or 4096 turns). Typical fits to the vertical profile are shown in Fig. **??**a at three different currents for bunch 23 of a 30-bunch train of positrons. Fig. **??**b shows the average bunch-by-bunch vertical beam sizes along a 30 bunch train at three bunch currents for the 30 bunch train at the low current of 0.5 mA/bunch, the vertical beam size is constant until the end of the train where a slow growth in the vertical beam size is noted. At the higher bunch currents of 0.75 and 1.0 mA/bunch, the slow growth starts near beginning of the train, with the bunch size growing more rapidly after bunch 20 for 0.75 mA/bunch, and bunch 14 for 1.0 mA/bunch.

For longer bunch trains, such as the 45 bunch train displayed in Fig. **??**c, similar behavior is noted. For the 0.5 bunch case a slow linear growth of the vertical beam size starts around bunch 24. At the higher bunch currents of 0.75 and 1.0 mA/bunch, a slow growth can be seen starting at the beginning of the train with the bunch size growing more rapidly after bunch 16 for 0.75 mA and bunch 12 for 1.0 mA. For both the 30 and 45 bunch trains their behavior is consistent with the cloud density increasing faster than linear along the train as bunch currents increase.

We define a âĂIJfast blow-up thresholdâĂİ as the bunch number, at which the rate of increase of the vertical beam size vs. bunch number begins to grow more rapidly than for the earlier bunches in the train.

As discussed above in Sec. **??** a synchrotron-betatron sideband signal is present from all bunches from the fast blow-up threshold to the end of the train. The beam size growth seen in Fig. **??**b and in Fig. **??**c before the fast blow-up threshold occurs around bunches 10-15 for both 30 and 45 bunch trains, may be due to incoherent emittance growth. The growth seen after the fast blow-up threshold may be due to both incoherent effects and the coherent instability.

When the feedback system is turned on the self-excitation signals that are observed in the multiple beam spectrum (MBS) results are suppressed by the feedback system. A consequence of turning the feedback system off while taking multiple bunch xBSM data is that bunches at the end of the bunch train have such large vertical dipole oscillations that they are not detected on the 32 pixel xBSM detector for all but a few turns. When large vertical dipole oscillations are detected, the vertical beam size can be determined by making cuts in the data but position and beam size spectra of these bunches are not understandable due to the lack of periodicity of the data.

In the case of the 45 bunch train at high current the head of the train was also seen to be enlarged. The cause of this is under investigation, but it is believed to be due to long-lived trapped electrons in the vacuum chambers within CESR. It should be noted that when the head of the train is enlarged a peak in the beam position spectrum is noticed at "V-1", as seen in Fig. **??**.

4.2 Vertical Chromaticity and Bunch Spacing Dependence

Measurements were made at three different vertical chromaticity settings at bunch spacings between 4 and 28 ns. The initial vertical chromaticity settings at each bunch spacing was determined by adjusting the chomaticity to its lowest value such that the 30 bunch train could be stored. The remaining two measurements were made at higher vertical chromaticity values. For these measurements the vertical feedback gains were set very low (20% nominal value) and the horizontal and longitudinal feedback was turned off. Two sets of measurements, one at 4 ns spacing (Fig. **??**) and 14 ns spacing (Fig. **??**), are shown. For the 4 ns spaced measurements the following observations were made:

- A large vertical dipole oscillations is evident when the vertical chomaticity is at its lowest setting as seen by plotting the turn-by-turn vertical centroid for bunch 27 in Fig. **??** . Raising the vertical chromaticity suppresses the dipole oscillations.

- The vertical beam size for the first two bunches in the train is large and correlates with the presence of a m=-1 head-tail line. Changing the vertical chromaticity does little to reduce either the head-tail line signal or vertical beam size. In addition the vertical centroid for the first three bunches is oscillating (Fig. **??**) and the chromaticity does not change the oscillation amplitude.

- Around bunch 15 the vertical beam size increases dramatically and the vertical chromaticity does not change the vertical beam size growth along the train.

- The reason for the insensitivity to chromaticity change is not known. It should be mentioned that the sideband amplitude was observed to change with chromaticity, as shown above in Sec. **??**.

For the 14 ns spaced measurements the following observations were made:

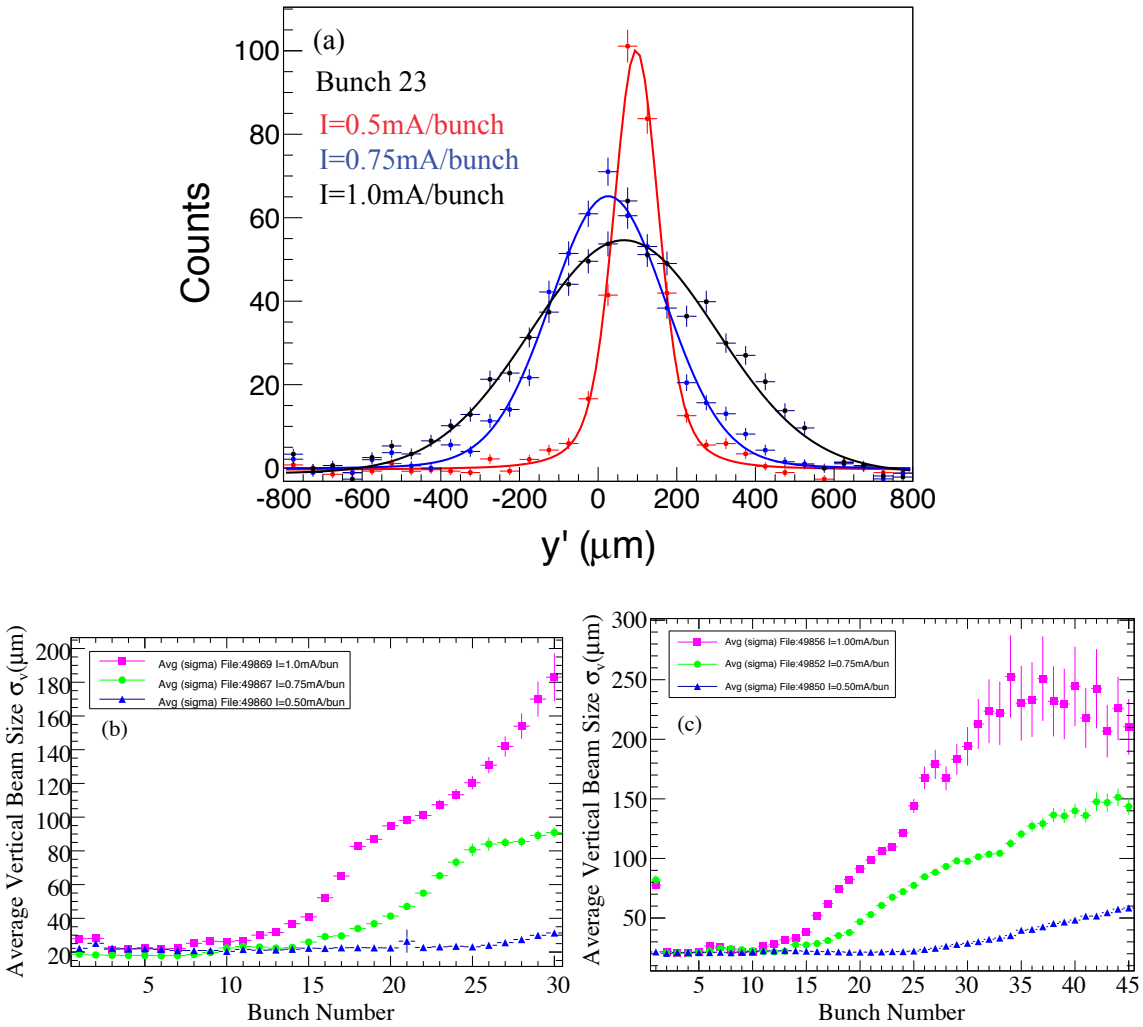

Figure 34. (a) Single bunch vertical bunch distribution of bunch 23 in a 30 bunch train of positrons at bunch currents of 0.5, 0.75, and 1 mA/bunch. As the bunch current is increased, the vertical beam size increases for bunch 23 in the 30 bunch train. (b) Average vertical beam size for 30 bunch train of positrons at three bunch currents. (c) Average vertical beam size for 45 bunch train of positrons at three different currents.

- Around bunch 10 the vertical beam size increases dramatically and the vertical chromaticity does not change the growth of the vertical beam size along the train.
- Toward the end of the train the vertical oscillation amplitude and size can vary depending on the vertical chromaticity (Fig. **??**). Increasing the vertical chromaticity reduces the ocillation amplitude for these bunches.

Since the vertical chromaticity does not change the blow-up threshold appreciably it is interesting to compare the vertical beam size along a 30 bunch train for bunch spacings between 4 to 28 ns as shown in (Fig. **??**). When changing from 4 ns spacing to 28 ns spacing above the beam size blow-up threshold, the rate of vertical beam size growth as bunch number increases changes from a rate at 12 ns bunch spacing to a more gradual blow up rate with bunch spacings of 20 ns

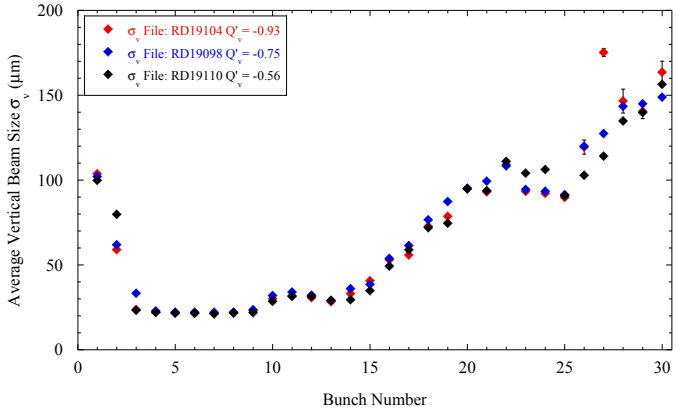

Figure 35. Bunch-by-bunch vertical beam size for 30 bunch positron train with 4 ns spacing and current of 0.75 mA/bunch.

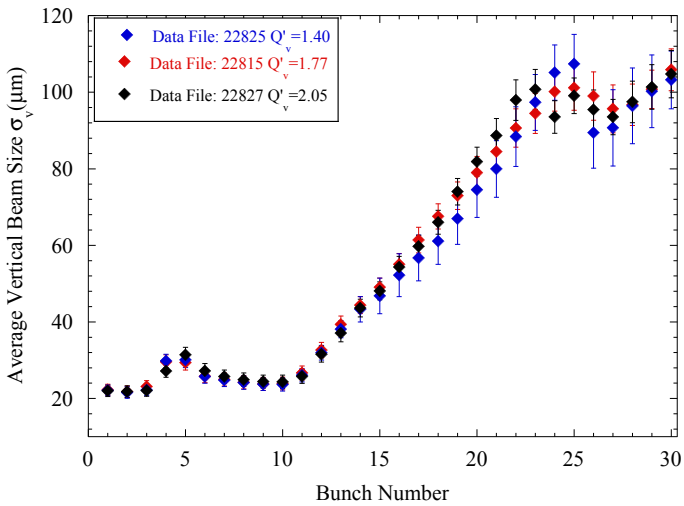

Figure 36. Bunch-by-bunch vertical beam size for 30 bunch positron train with 14 ns spacing and current of 0.75 mA/bunch.

or greater. The change in the blow-up threshold and slope may be due to the cloud lifetime being long compared to the bunch spacing and so the cloud does not decay appreciably over the space of 14 ns, allowing the cloud density to become a function of the number of preceding bunches.

4.3 Emittance Dependence

The initial beam size at CESR was varied by changing the vertical emittance of the ring with a 30 bunch train of positrons at 0.6 mA/bunch and feedback turned on. The vertical beam size was measured at three enlarged vertical emittances and is compared to the nominal emittance value with the results shown in Figure **??** (a). The beam size growth along the train, when the vertical emittance is increased, behaves in a similar manner for all four vertical emittances indicating that the threshold is similar. By plotting the vertical beam size relative to the first bunch in the train

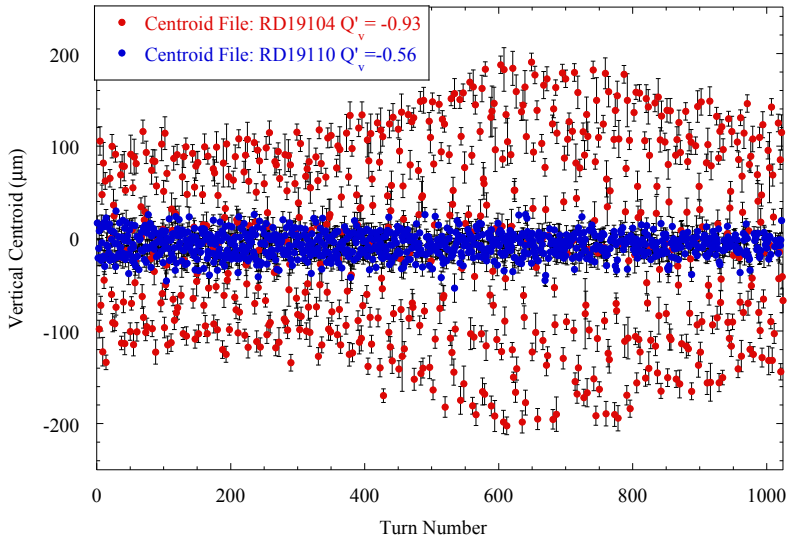

Figure 37. Bunch 27 of a 30 bunch train vertical beam motion over 1024 turns when bunch spacing was 4 ns and 0.75 mA/bunch at two different vertical chromaticites.

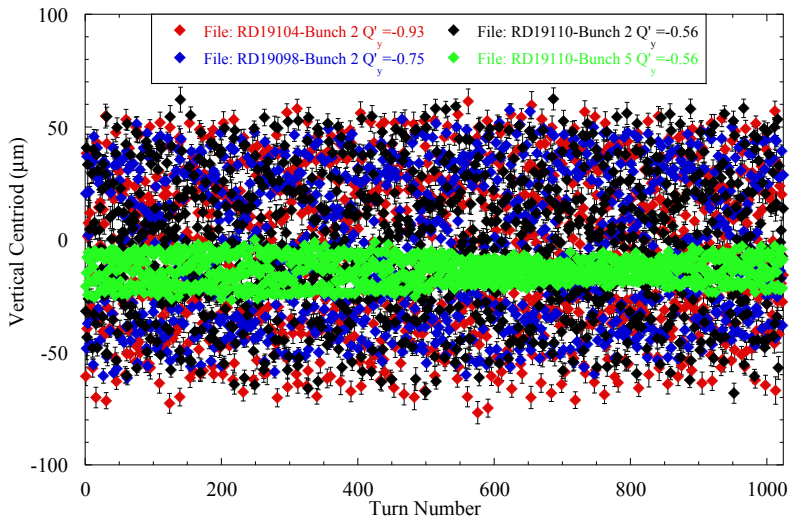

Figure 38. The vertical centroid motion over 1024 turns for bunch 2 at three different chromaticities and Bunch 5 at a single chromaticity for a 30-bunch train with 4 ns bunch spacing and a single bunch current of 0.75 mA/bunch.

(Figure **??**(b)), it is evident that the vertical beam size growth threshold is relatively independent of the storage ring's emittances.

The reason for the lack of dependence of the threshold on the vertical beam size can be seen from the electron cloud density expression [**?**]

$$\rho_{e,th} = \frac{2\gamma\nu_s}{\sqrt{3}\mathrm{Min}(Q_{nl},\chi)r_e\beta_y L}. \tag{4.1}$$

The phase factor χ is 9.5 for CESR at 2.1 GeV, which is larger than the numerically estimated

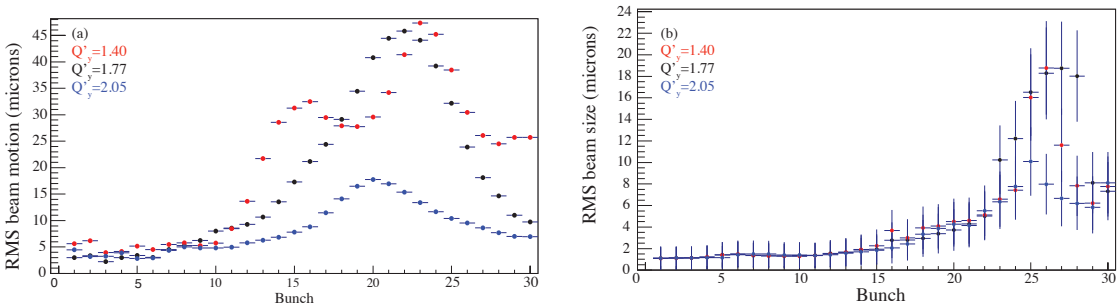

Figure 39. (a) The RMS beam motion (b) RMS beam size along the 30-bunch train with 14 ns spacing at three different vertical chromaticities.

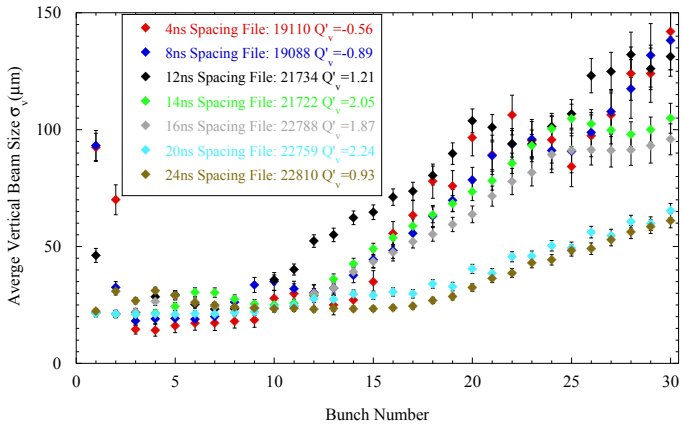

Figure 40. Bunch-by-bunch beam size for 30 bunch train of positrons at 0.75 mA/bunch and bunch spacing's ranging from 4-28 ns.

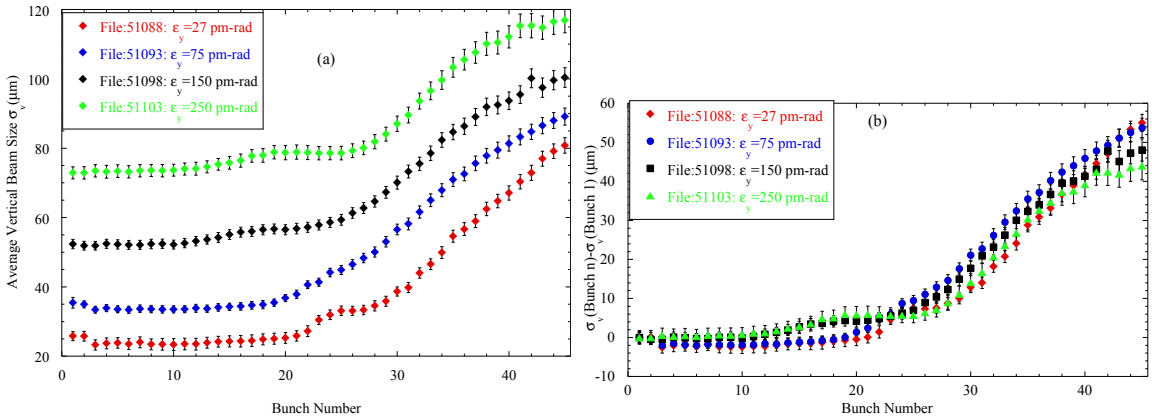

Figure 41. Bunch-by-bunch vertical beam size for a 45 bunch train with 14 ns spacing and 0.6 mA/bunch with (a) four different emittance's, and (b) four different emittanes where the vertical beam size is plotted relative to the first bunch in the train.

natural $Q_{nl} \sim 7$ for a coasting beam [?]. In this case the threshold is independent of vertical beam size (for small changes in the beam size).

4.4 Feedback Gain Dependence

CESR presently contains two independent transverse and longitudinal feedback systems: 1) The original systems capable of damping bunches with a spacing of 14 ns [?],[?],[?] and 2) a commercial system by Dimtel, which can damp bunches with a spacing as small as 4 ns [?]. Figure ?? shows the result of a study for the effect of the first of these two feedback systems for two different settings of the transverse feedback gain at CesrTA : 20% and 40% of full scale gain settings, for both vertical and horizontal feedback. While the damping rate of the dipole mode changes with the feedback gain, the characteristics of the vertical beam size blow-up behavior is not affected at all.

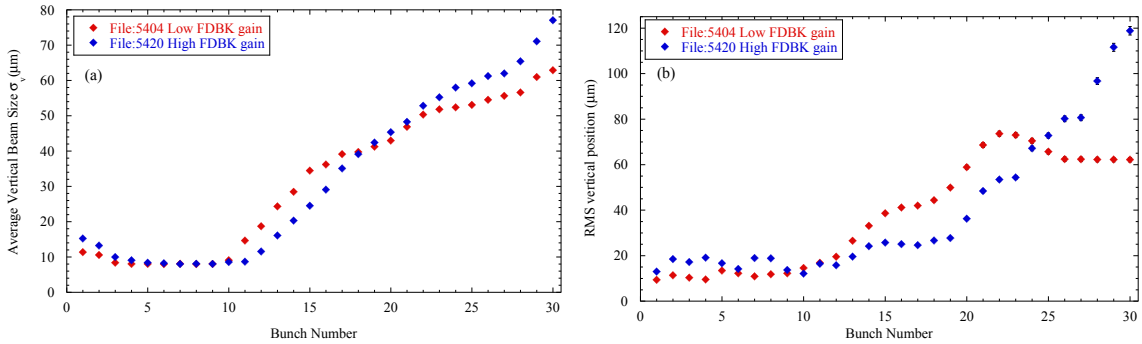

Figure 42. Bunch-by-bunch vertical (a) beam size and (b) rms motion for 30 bunch train with 14 ns spacing with 0.75 mA/bunch as feedback gain is varied from 20% and 40% of full scale.

4.5 Comparison with Bunch-by-Bunch Frequency Spectra

In Fig. ?? the bunch-by-bunch beam size and rms motion are shown for a measurement with a 14 ns train, at 4 GeV, with 1.1 mA/bunch. The measurements were taken concurrently with those for the bunch-by-bunch frequency measurement described in Sec. ??. For that measurement the growth of the vertical head-tail lines are shown in Fig. ??. The $m = 1$ vertical head-tail line starts growing at bunch 18 and peaks around bunch 22. Comparing with Fig. ?? the vertical emittance growth starts at bunch 17 and reaches a plateau around bunch 22. Thus the onset and development along the train of the vertical head-tail lines is very similar to the onset and development along the train of vertical emittance growth.

4.6 Summary

Using an x-ray monitor, bunch-by-bunch vertical size and position measurements have been made on a turn-by-turn basis to study the evolution of the beam emittance along trains of bunches in the presence of the electron cloud. The following observations have been made from these measurements:

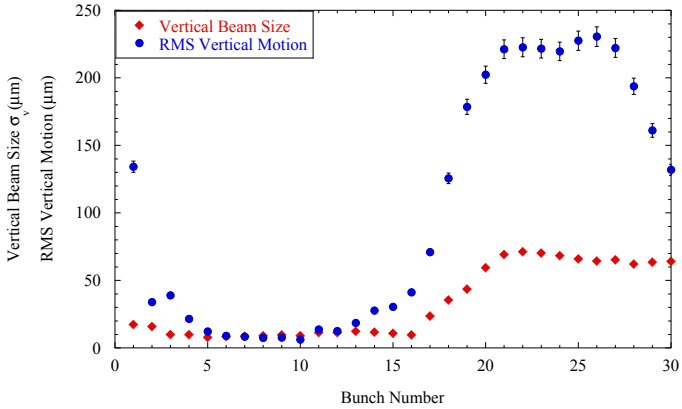

Figure 43. Bunch-by-bunch beam size and rms motion at 14 ns, 4 GeV, with 1.1 mA/bunch.

- Vertical beam size growth is observed along bunch trains where the growth rate vs. bunch number is a strong function of the bunch current (see Fig. **??**). The first bunch in the train can have an anomalously larger size, which correlates with of the observation of the emergence of a vertical head-tail line in the spectrum for this bunch, as discussed in Sec. **??**.
- Vertical beam size growth along the train is not very sensitive to the chromaticity (see Fig. **??**).
- Changing the spacing between bunches has a relatively small effect on the vertical beam size growth along the train for spacings less than 20 ns. However, when the bunch spacing is 20 ns or greater, the beam size growth rate for later bunches in the train drops considerably (see Fig. **??**).
- Beam size growth along the train is also not very sensitive to the initial beam size or the feedback gain (see Figure **??** and Figure **??**).
- The onset and development along the train of the vertical head-tail lines is very similar to the onset and development along the train of vertical emittance growth (compare Fig. **??** and Fig. **??**).

5 Conclusions

We have described the experimental measurements performed at CESR which probe the interaction of the electron cloud with the stored beam. These experiments have been done over a wide range of beam energies, emittances, bunch currents, and fill patterns to gather sufficient information to begin to characterize the beam-electron-cloud interaction and will be useful for comparing with the simulation software. The beam conditions are chosen to be as close as possible to those of the ILC damping rings, with enough variation in the conditions that we have some confidence in being able to extrapolate to the ILC dampings. This data can be employed for the validation of the simulation programs, allowing more accurate predictions for the cloud-related behavior of exsisting and future storage and damping rings.

Acknowledgments

These experiments would not have been possbile without the support of the CESR Opaerations Group. This work was supported by DOE Award DE-FC02-08ER41538, NSF Award PHY-0734867, PHY-1068662, PHY-1535696 and the Lepton Collider Research and Development, Coop Agreement: NSF Award PHY-1002467.

References

[1] Palmer M A, Alexander J, Billing M, Calvey J, Chapman S, Codner G, Conolly C, Crittenden J, Dobbins J, Dugan G, Fontes E, Forster M, Gallagher R, Gray S, Greenwald S, Hartill D, Hopkins W, Kandaswamy J, Kreinick D, Li Y, Liu X, Livezey J, Lyndaker A, Medjidzade V, Meller R, Peck S, Peterson D, Rendina M, Revesz P, Rice D, Rider N, Rubin D, Sagan D, Savino J, Seeley R, Sexton J, Shanks J, Sikora J, Smolenski K, Strohman C, Temnykh A, Tigner M, Whitney W, Williams H, Vishniakou S, Wilksen T, Harkay K, Holtzapple R, Smith E, Jones J, He Y, Ross M, Tan C Y, Zwaska R, Flanagan J, Jain P, Kanazawa K, Ohmi K, Sakai H, Shibata K, Suetsugu Y, Byrd J, Celata C M, Corlett J, De Santis S, Furman M, Jackson A, Kraft R, Munson D, Penn G, Plate D, Rawlins A, Venturini M, Zisman M, Kharakh D, Pivi M and Wang L 2009 The conversion and operation of the cornell electron storage ring as a test accelerator (cesrta) for damping rings research and development *Proceedings of the 2009 Particle Accelerator Conference, Vancouver, BC* pp 4200–4204 URL http://accelconf.web.cern.ch/AccelConf/PAC2009/papers/fr1rai02.pdf

[2] Billing M G, Dugan G, Forster M J, Meller R E, Palmer M A, Ramirez G A, Sonnad K, Sikora J P, Williams H A and Holtzapple R L 2011 Measurement techniques to characterize instabilities caused by electron clouds *Proceedings of the 2011 Particle Accelerator Conference, New York, NY* pp 1852–1854 URL http://accelconf.web.cern.ch/AccelConf/PAC2011/papers/wep194.pdf

[3] Billing M G, Dugan G, Meller R, Palmer M, Rendina M, Rider N, Sikora J, Strohman C and Holtzapple R L 2010 Techniques for observation of beam dynamics in the presence of an electron cloud *Proceedings of the 2010 International Particle Accelerator Conference, Kyoto, Japan* pp 1197–1199 URL http://accelconf.web.cern.ch/AccelConf/IPAC10/papers/mope091.pdf

[4] Shanks J, Rubin D L, Crittenden J and Palmer M 2012 Characterization of single particle dynamics for the international linear collider damping ring lattice *Proceedings of the 2012 International Particle Accelerator Conference, New Orleans, LA* pp 1972–1974 URL http://accelconf.web.cern.ch/accelconf/IPAC2012/papers/tuppr066.pdf

[5] Rider N T, Alexander J P, Dobbins J A, Billing M G, Meller R E, Palmer M A, Peterson D P, Strohman C R and Flanagan J W 2011 Development of an x-ray beam size monitor with single pass measurement capability for cesrta *Proceedings of the 2011 Particle Accelerator Conference, New York, NY* pp 687–689 URL http://accelconf.web.cern.ch/AccelConf/PAC2011/papers/mop304.pdf

[6] Billing M, Butler K, Dugan G, Forster M, Ramirez G *et al.* 2014 Recent results for the dependence of beam instabilities caused by electron clouds at cesrta due to variations in bunch spacing and chromaticity p TUPRI067

[7] Arduini G, Cornelis K, Höfle W, Rumolo G and Zimmermann F 2003 The elelctron cloud instability of the lhc beam in the cern sps

[8] Kreinick D L, Crittenden J A, Dugan G, Palmer M A, Ramirez G, Holtzapple R L, Randazzo M, Furman M A and Venturini M 2011 Application of coherent tune shift measurements to the

characterization of electron cloud growth *Proceedings of the 2011 Particle Accelerator Conference, New York, NY* pp 1680–1682 URL http://accelconf.web.cern.ch/AccelConf/PAC2011/papers/wep108.pdf

[9] Dugan G, Billing M, Butler K, Crittenden J, Forster M, Kreinick D, Meller R, Palmer M, Ramirez G, Rendina M, Rider N, Sonnad K, Williams H, Chu J, Campbell R, Holtzapple R, Randazzo M, Flanagan J, Ohmi K, Furman M, Venturini M and Pivi M 2012 Studies at cesrta of electron-cloud-induced beam dynamics for future damping rings *Proceedings of the 2012 International Particle Accelerator Conference, New Orleans, LA* pp 2081–2085 URL http://accelconf.web.cern.ch/accelconf/IPAC2012/papers/weya02.pdf

[10] Flanagan J W, Ohmi K, Fukuma H, Hiramatsu S, Tobiyama M and Perevedentsev E 2005 *Phys. Rev. Lett.* **94**(5) 054801 URL http://link.aps.org/doi/10.1103/PhysRevLett.94.054801

[11] Flanagan J W, Ohmi K, Fukuma H, Funakoshi Y, Hiramatsu S, Ieiri T, Ikeda H, Oide K and Tobiyama M 2006 Further studies on betatron sidebands due to electron clouds *Proceedings of the 2006 European Particle Accelerator Conference, Edinburgh, Scotland* pp 2898–2900 URL http://accelconf.web.cern.ch/AccelConf/e06/PAPERS/THPCH050.PDF

[12] Palmer M A, Billing M G, Calvey J R, Codner G W, Greenwald S, Li Y, Liu X, Livezey J A, Meller R E, Schwartz R M, Sikora J P, Strohman C R, Whitney W S and Wilksen T 2009 Design, implementation and first results of retarding field analyzers developed for the cesrta program *Proceedings of the 2009 Particle Accelerator Conference, Vancouver, BC* pp 3510–3512 URL http://accelconf.web.cern.ch/AccelConf/PAC2009/papers/th5rfp030.pdf

[13] Peterson D P, Alexander J P, Conolly C, Eggert N, Fontes E, Hopkins W, Kreis B, Lyndaker A, McDonald M, Palmer M, Rendina M, Revesz P, Rider N, Savino J, Seeley R and Flanagan J W 2010 Cesrta x-ray beam size monitor operation *Proceedings of the 2010 International Particle Accelerator Conference, Kyoto, Japan* pp 1194–1196 URL http://accelconf.web.cern.ch/AccelConf/IPAC10/papers/mope090.pdf

[14] Alexander J, Chatterjee A, Conolly C, Edwards E, Ehrlichman M *et al.* 2014 *Nucl.Instrum.Meth.* **A748** 96–125 (*Preprint* 1311.6769)

[15] Palmer M A, Billing M G, Dugan G F, Furman M A and Rubin D L Jan 2013 The cesr test accelerator electron cloud research program: Phase i report Tech. rep. LEPP, Cornell University, Ithaca, NY

[16] Ohmi K, Zimmermann F and Perevedentsev E 2001 *Phys. Rev. E* **65** 016502

[17] Sikora J, Billing M, Codner G, Meller R, Strohman C and Pelaia T 1999 Longitudinal feedback at cesr *Proceedings of the 1999 Particle Accelerator Conference, New York, NY* ed Luccio A and MacKay W pp 1115–1117 URL http://accelconf.web.cern.ch/AccelConf/p99/PAPERS/TUA19.PDF

[18] Rogers J T, Billing M G, Dobbins J A, Dunnam C R, Hartill D L, Holmquist T, McDaniel B D, Pelaia T A, Pisharody M, Sikora J P and Strohman C R 1995 Operation of a fast digital transverse feedback system in cesr *Proceedings of the 1995 Particle Accelerator Conference, Dallas, TX* pp 2426–2428 URL http://accelconf.web.cern.ch/AccelConf/p95/ARTICLES/RAE/RAE14.PDF

[19] Billing M, Codner G, Hartill D, Meller R, Sikora J and Vescherevich V 2001 Performance of the beam stabilizing feedback systems at cesr *Proceedings of the 2001 Particle Accelerator Conference, Chicago, IL* ed Lucas P and Webber S pp 1243–1245 URL http://accelconf.web.cern.ch/AccelConf/p01/PAPERS/TPAH006.PDF

[20] Teytelman D 2009 igp-1281f signal processor: Technical user manual, revision 1.7 Tech. rep. Dimtel, Inc. San Jose, CA URL http://www.dimtel.com/_media/support/manuals/manual_1281f.pdf